Estimating the age and growth of bigeye tuna (*Thunnus obesus*) in the Indian Ocean from counts of daily and annual increments in otoliths

Jessica Farley[1], Kyne Krusic-Golub[2], Paige Eveson[1], Naomi Clear[1], Patricia L. Luque[3], Iraide Artetxe-Arrate[3], Igaratza Fraile[3], Iker Zudaire[3], Annie Vidot[4], Rodney Govinden[4], Ameer Ebrahim[4], Evgeny Romanov[5], Emmanuel Chassot[6,7], Nathalie Bodin[6,8], Denham Parker[9], Hilario Murua[10], Francis Marsac[11], Gorka Merino[3]

[1] CSIRO Oceans and Atmosphere, Hobart, Australia; jessica.farley@csiro.au

[2] Fish Ageing Services Pty Ltd, Victoria, Australia; kyne.krusicgolub@fishageingservices.com

[3] AZTI, Marine Research, Basque Research and Technology Alliance (BRTA), Pasaia, Gipuzkoa, Spain; gmerino@azti.es

[4] Seychelles Fishing Authority, Victoria, Seychelles; rgovinden@sfa.sc

[5] CAP RUN - CITEB (Centre technique de recherche et de valorisation des milieux aquatiques), Île de la Réunion; evgeny.romanov@ird.fr

[6] Research Institute for Sustainable Development (IRD), Victoria, Seychelles

[7] IOTC Secretariat, Victoria, Seychelles; Emmanuel.Chassot@fao.org

[8] South African Department of Environment, Forestry and Fisheries (DEFF), Cape Town, South Africa; denhamparker@gmail.com

[9] Sustainable Ocean Seychelles (SOS), Beau Belle, Seychelles; natbod@gmail.com

[10] International Seafood Sustainability Foundation, Washington DC, USA; hmurua@iss-foundation.org

[11] Research Institute for Sustainable Development (IRD), UMR MARBEC, Victoria, Seychelles; francis.marsac@ird.fr

Executive summary

This paper describes work to estimate the age and growth of bigeye tuna (*Thunnus obesus*) in the Indian Ocean from otoliths as part of the 'GERUNDIO' project[1]. The most recent stock assessment for Indian Ocean bigeye tuna indicated that the stock is not overfished but overfishing is occurring (Fu 2019; IOTC 2020). The stock assessment model used a fixed growth function from Eveson et al. (2012), which was estimated using tag-recapture data and daily age estimates from otoliths. A slightly updated (but very similar) growth curve was

[1] Collection and analysis of biological samples of tropical tunas, swordfish, and blue shark to improve age, growth and reproduction data for the Indian Ocean Tuna Commission (IOTC), FAO Contract No. 2020/SEY/FIDTD/IOTC - CPA 345335.

presented in Eveson et al. (2015), which suggests a two-stanza growth model for bigeye tuna where growth is slow for fish between 40 and 50 cm fork length (FL), then changes to faster growth between 50 and 70 cm FL, before slowing again. The otolith-based daily age estimates from Sardenne et al. (2015) that were used in the analysis varied considerably among readers and there was a recommendation by Sardenne et al. (2015) to explore alternate ageing methods, such as annual ageing (as opposed to daily ageing). More recently, Farley et al. (2017; 2020) developed a new method to estimate the decimal age of bigeye tuna in the western and central Pacific Ocean from validated counts of daily and annual growth zones in otoliths. The aim of the current study was to apply this method to bigeye tuna in the Indian Ocean to obtain new estimates of age and growth, and to attempt to validate the age estimates using otoliths from bigeye tuna tagged and recaptured in the Indian Ocean Tuna Tagging Programme (IOTTP).

Otoliths from 632 bigeye tuna collected in the current and previous projects were available for analysis and otoliths from 108 fish were selected for ageing. The otoliths were collected from bigeye tuna ranging in size from 18.5 to 178 cm FL. A combination of daily and annual ageing was undertaken, and a final age was obtained for 107 of the 108 fish. The youngest fish was aged 49 days and the oldest was 14.7 years. The preliminary age validation/ verification work using otoliths and data from the IOTTP provides evidence that the otolith ageing method used in this study is accurate. However, we recommend that further age validation work is undertaken.

Three growth models were fit to the age and length data (VB, Richards and VB log k). All three provided very similar fits; however, the two-phase VB log k model provided a better fit to the data for fish <40 cm FL. The length-at-otolith weight data (which is independent of the age estimation method) showed a change in otolith growth at ~40 cm FL consistent with the length-at-age data, which lends support to the VB log k model. Overall, our analysis shows that growth is rapid in the first few years with fish reaching ~60 cm FL at age 1 and ~85 cm FL at age 2. Mean asymptotic length was estimated to be ~168 cm FL.

The VB log k growth curve estimated in the current study is similar to the VB curve of Stéquert and Conand (2004) for bigeye tuna in the western Indian Ocean, which was estimated using counts of microincrements (daily age estimates) in otoliths, although we obtained higher age estimates for fish >140 cm FL. Also, our VB log k curve suggests faster growth for fish up to ~40 cm FL.

Although our data suggests two-phase growth, our VB log k growth curve is quite different from the integrated VB log k curves of Eveson et al. (2012; 2015). In particular, we do not see the same very slow growth for fish < 50 cm, plus we estimate mean asymptotic length to be higher (~168 cm FL in the current study compared to 152.5 cm FL in Eveson et al. 2015). This may be due to the low number of fish >150 cm FL in the tag-recapture data available at the time to be used in Eveson et al. (2015), which is likely related to the relatively short times at liberty of fish included in the analysis (<6 years) compared to the current estimated longevity of bigeye tuna of at least 14 years.

We recommend that additional otoliths are collected from the eastern Indian Ocean, and that these otoliths and additional otoliths from those already collected in the GERUNDIO and IOTTP projects are read/aged to provide further information on growth and longevity before the next stock assessment for bigeye tuna in 2022.

1. Introduction

Bigeye tuna (*Thunnus obesus)* is a large pelagic species inhabiting tropical and subtropical waters in all the major oceans. Genetic studies indicate that bigeye tuna form a single stock in the Indian Ocean, which is not connected to stocks in the Pacific or Atlantic Oceans (Appleyard et al. 2002; Chiang et al. 2008; Díaz-Arce et al. 2020). In 2019, the stock assessment for bigeye tuna in the Indian Ocean indicated that the stock is not overfished but overfishing is occurring, and the spawning stock biomass in 2018 was estimated at 31% of the unfished levels (Fu 2019; IOTC 2020). The next assessment of bigeye tuna is planned to be conducted in 2022.

Accurate life-history parameters such as age and growth are required for robust stock assessments and management advice. The 2019 stock assessment model for bigeye tuna used a fixed growth function from Eveson et al. (2012), which was estimated using tag-recapture data from the Indian Ocean Tuna Tagging Programme (IOTTP; Murua et al. 2015) and otolith-based daily age estimates from Sardenne et al. (2015). A slightly updated growth curve was presented in Eveson et al. (2015), but is very similar to that in Eveson et al. (2012). Mean asymptotic length was estimated to be 150.9 cm FL in Eveson et al. (2012), and 152.5 cm FL in Eveson et al. (2015). The tag-recapture data was more influential in the growth models than the direct age data due to the volume of tagging data, and the results indicated that bigeye tuna have a two-stanza growth pattern where growth was slow for fish between 40 and 50 cm FL, then changed to faster growth between 50 and 70 cm FL, before slowing again (Eveson et al. 2012; 2015). The daily age estimates used by Eveson et al. (2015) varied considerably among readers and hence there was a recommendation by Sardenne et al. (2015) to explore alternate ageing methods uding otolthis, such as annual ageing (as opposed to daily ageing).

In 2020, the European Union and the Indian Ocean Tuna Commission (IOTC) supported the 'GERUNDIO' project for the "*collection and analysis of biological samples of tropical tunas, swordfish, and blue sharks to improve age, growth and reproduction data for the IOTC*". One of the objectives of the project was to develop new estimates of age and growth for bigeye tuna in the Indian Ocean. The aim was to follow methods recently developed by Farley et al. (2017; 2020) for bigeye tuna in the Western Central Pacific Ocean (WCPO) to estimate the age and growth of bigeye tuna from counts of daily and annual growth zones in otoliths. In addition, a priority for the project was to undertake preliminary age validation by analysing otoliths from bigeye tuna that had been tagged and recaptured in the IOTTP.

2. Methods

2.1. Sample collection and selection for ageing

Sagittal otoliths from 632 bigeye tuna were available for analysis (as of 1 October 2021). Of these, otoliths from 98 (15%) fish were collected in the current project in the western Indian Ocean in 2021. The remaining otoliths were made available from the "*Estimation of Maternal effects upOn the sustainability of large pelagic populaTIONs*" (EMOTION) and "*Population Structure of Tuna, Billfish and Sharks in the Indian Ocean*" (PSTBS-IO) projects (Bodin et al. 2018, Davies et al. 2020) and were collected between 2013 and 2018 across the Indian Ocean. Figure 1 shows the sampling locations for all otoliths divided into those aged and not aged. Straight fork length (FL) was measured to the nearest cm for all fish. Sex data were available for 273 fish (43% of the total number of fish).

The otoliths were cleaned, dried, and weighed to the nearest 0.0001 g if complete. A total of 108 fish were selected for ageing based on fish length and sampling location to ensure age estimates were obtained from length classes where sample sizes were small and from across the spatial range of fish sampled. Figure 2 shows the size frequency of fish selected for ageing and those remaining in the archive for future analysis.

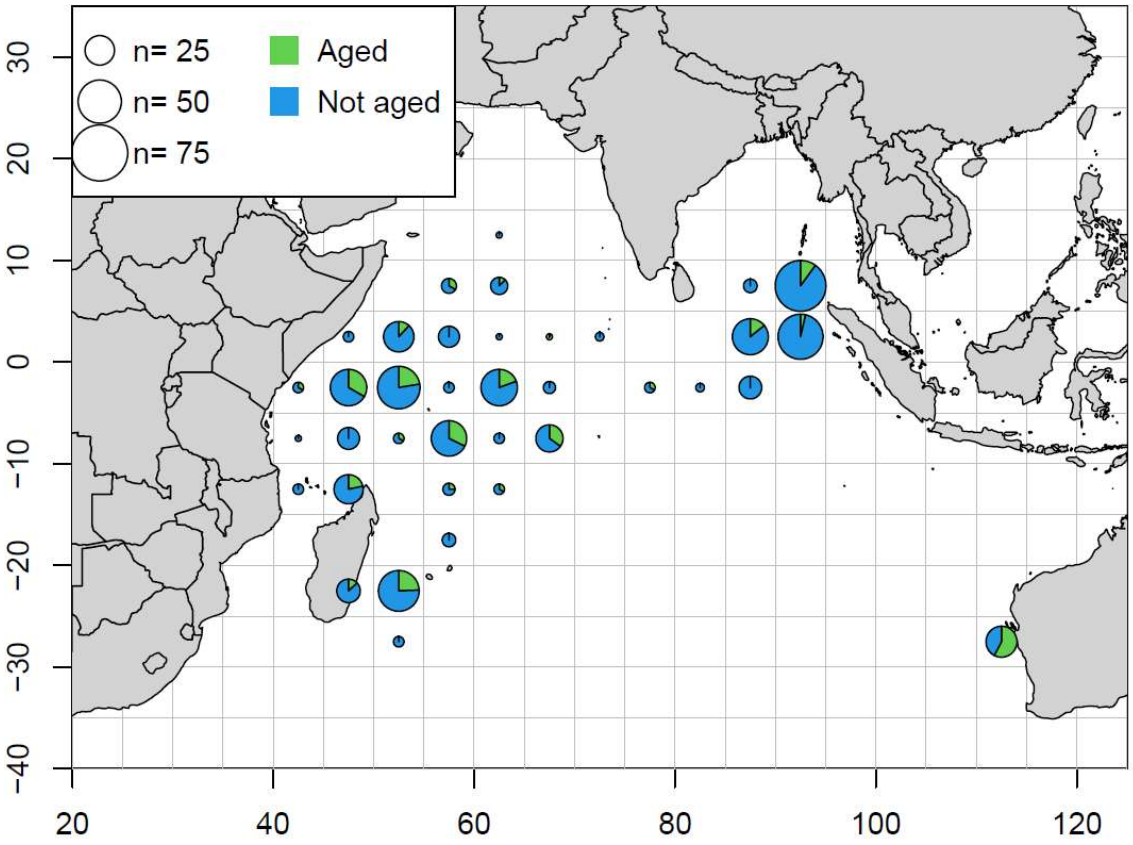

Figure 1. Map of the sampling locations for bigeye tuna. Circle size is proportional to sample size, and colours indicate the proportion of otoliths that have been aged and are included in the growth analysis (green) and the proportion remaining in the collection for future analysis (blue). Note that specific location information

was not available for 57 samples collected in the northwest Indian Ocean, so were not included in the map. Longitude is shown in degrees east.

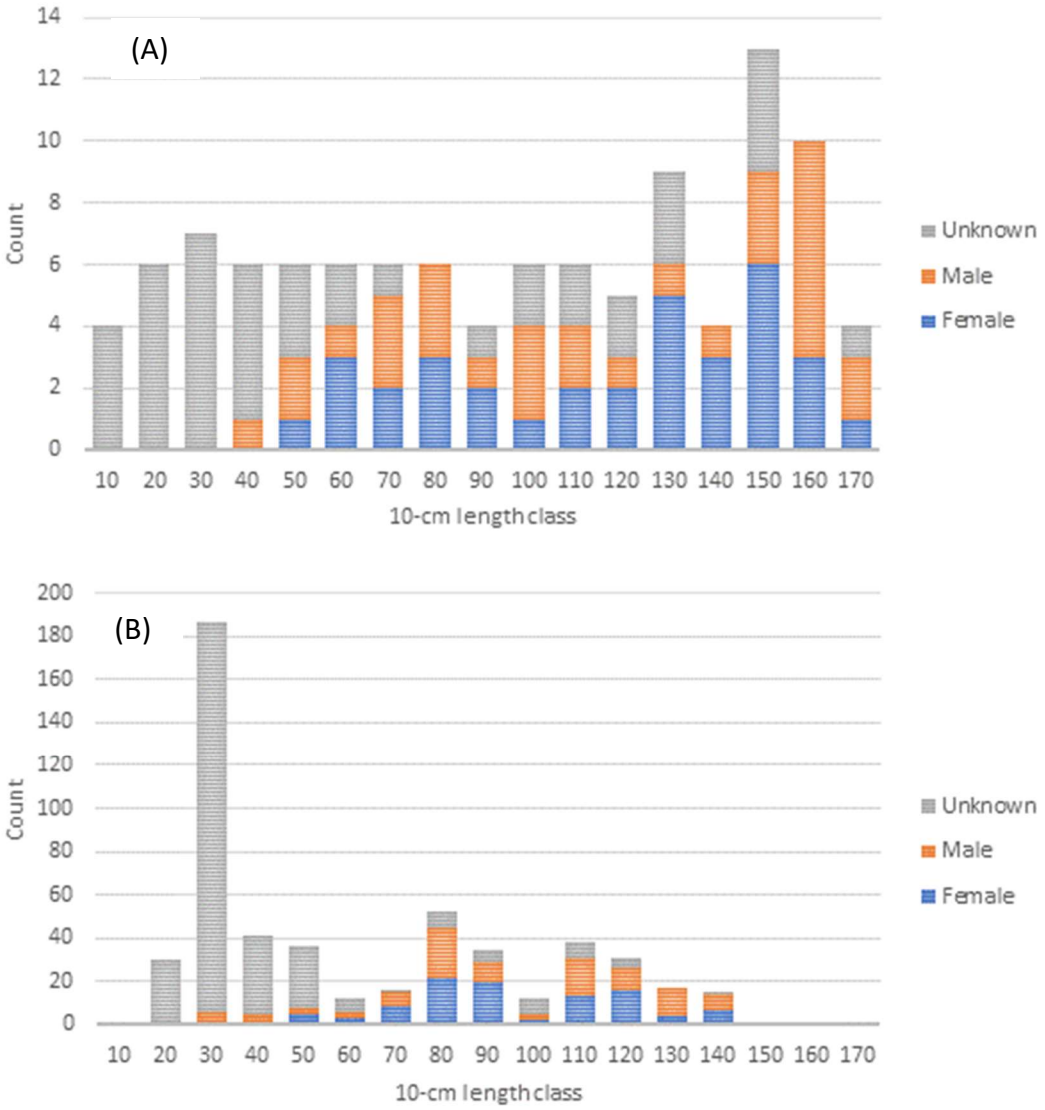

Figure 2. Length frequency (FL) of bigeye tuna (A) selected for ageing and included in the preliminary growth analysis for the Indian Ocean in this study (n=108), and (B) the remaining samples in the collection from the Indian Ocean (n=524). The lower boundary length value of the bin is shown.

2.2. Otolith preparation and reading

Both daily and annual increments were examined in this study following methods developed for bigeye tuna in the WCPO (Farley et al. 2017; 2020).

Daily ageing

A total of 39 otoliths were prepared for daily age reading: 37 were selected from small fish (18.5-79.0 cm FL), and two additional otoliths were selected from larger fish (82.5 and 82.9

cm FL) to determine if a daily age could be obtained with confidence. The method involves preparing single longitudinal (frontal) sections from the primordium to the postrostral axis of the otolith, through the primordium (Williams et al. 2013). The number of visible microincrements (assumed daily growth zones) were counted from the primordium to the terminal edge of the section under high magnification on a compound microscope. All otoliths were prepared and read by Fish Ageing Services Pty Ltd (FAS) in Australia. Each sample was read twice by the same reader and if the difference in counts was >10%, then a third reading was completed. The average of the two closest readings was used as the final count.

An additional sub-sample of nine transverse sections used in the Sardenne et al. (2015) study was selected for re-reading. Microincrements were counted using a transmitted light microscope at various magnifications ranging between 400 and 1000x depending on the area of the otolith being interpreted. The reading transects in this study varied slightly from that used in the Sardenne et al. (2015) study (see Figure 3), where zones were initially counted closer to the sulcal edge rather than the outer edge of the otolith.

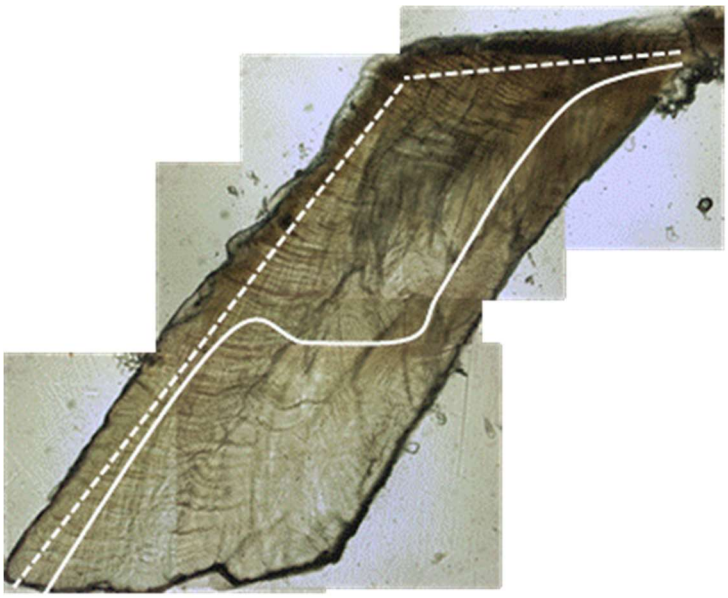

Figure 3. Image of a transversely prepared otolith section for daily age reading showing the reading path used by Sardenne et al. (2015) (dashed line) and that used in this study (solid line)

Annual ageing

A total of 103 otoliths were selected from fish 71-178 cm FL for annual age reading (34 were sister otoliths of those prepared for daily age estimation above). The otoliths were prepared following the methods outlined in Anon (2002). Otoliths were embedded in clear casting polyester resin and four or five serial sections approximately 300 μm thick were cut from each otolith (around the primordium). Sections from each sample were cleaned, dried, and mounted on glass microscope slides (50 × 76 mm) with resin. Sections were then covered with further resin and two glass coverslips (22 × 60 mm) were placed side by side. All otoliths were

prepared by FAS and read once by an experienced reader at FAS and once by an experienced reader CSIRO, using a dissecting microscope and transmitted light. FAS used an image analysis system to read the sectioned otoliths. The system counts and measures the distance of each manually marked opaque zone from the primordium and collects an annotated image from each sample read (see Figure 9 below). The opaque zones at the terminal edge of the otolith were only marked if they were complete and some translucent material was evident after the opaque zone. The otolith edge was classified as new opaque, narrow translucent or wide translucent based on the criteria developed for Pacific bigeye tuna otoliths (Farley et al. 2017) and each reading was assigned a confidence score of 0-5 (poor-good). CSIRO read the otolith sections using the method described above but did not use an image analysis system to obtain an image of the otolith or measure the increments. Average percent error (Beamish and Fournier 1981) and age difference tables were used to assess the precision of readings. When counts differed, the FAS count was used for the fish.

Decimal age was calculated for each fish with an annual count based on the method developed for bigeye tuna and yellowfin tuna (*Thunnus albacares*) in the western Pacific Ocean (Farley et al. 2020).

First, the age of each fish when the first opaque zone was completed in the transverse section was calculated. This was done using the relationship between daily age and otolith size for paired otoliths (Append Figure 1). Daily age estimates were obtained from the longitudinal sections (as described in previous section "Daily ageing") and otolith size was the measurement from the primordium to the distal edge of the first opaque zone on the transverse section of the 'sister' otolith prepared for annual ageing. The daily age-otolith size relationship was estimated using a power curve (Append Figure 1).

Second, the number of complete annual increments in the otolith was calculated. A complete annual increment is one opaque zone plus one translucent zone, which represents presumably one year of growth, and is calculated as the total count of opaque zones minus 1.

Third, the time elapsed after the last counted opaque zone was deposited and when the fish was caught was estimated. This was calculated using the width of the marginal increment in the otolith prepared as a proportion of the mean width of the complete annulus for that age group (see Append Figure 2). The mean increment width was calculated using the otolith measurements taken routinely for each otolith included in the annual ageing. The distance between the terminal edge of each opaque zone was calculated, and the mean width estimated for each age group.

The total age of each fish was estimated by adding together the age components estimated in each of these three steps. Note that for otoliths less than 1.4 mm in size (i.e., within the range of the power curve in Append Figure 1), age was estimated using only the otolith measurement (i.e., only step 1).

2.3. Annual age validation and verification

Otoliths from IOTTP tag-recapture bigeye tuna

Preliminary age validation for bigeye tuna was undertaken using otoliths from fish that had been tagged and recaptured as part of the IOTTP and were at liberty for up to 6.8 years. A total of 91 otoliths were sent to FAS where they were weighed to the nearest 0.001 g if complete.

A subset of the otoliths was selected for annual ageing by FAS, which consisted of (1) five OTC marked samples ranging from 0.90 to 3.19 years at liberty and 75 to 141 cm FL length at recapture, and (2) 10 non-OTC marked samples ranging from 3.75 to 6.80 years at liberty and 41 to 157 cm FL at recapture. Transverse sections were prepared using the same method as described in section 2.2. The only modification was that during the processing of the OTC samples, the blocks and slides were not subject to heat and were stored in a dark box while the resin cured as both heat and direct light can reduce the intensity of the OTC mark prior to examination

Otoliths marked with OTC were examined for the presence and position of the OTC mark using a Leitz Diaplan compound microscope fitted with a 100-W incident ultraviolet light source, and a Leitz D filter block (excitation filter 450–520 nm) to suit the fluorescent properties of OTC. One image was captured of the otolith under fluorescent illumination and another under transmitted light for direct comparison.

Since the time at liberty was known for each fish (i.e., a truly blind read was not possible at this time), we used an objective method to verify the annual age estimation method used in this study. For each of the 15 sectioned otoliths, we measured the distance from the primordium to the otolith edge on the counting path. We then estimated the age of the fish at recapture by summing the estimated age of the fish when it was tagged (using its length measurement and the relationship in Figure 4) and the time at liberty. All fish were <70 cm FL at release so were within the range used in developing the relationship in Figure 4. We compared the relationship between age and the size of the sectioned otolith to the same information from the otoliths of all bigeye tuna aged in this study, to determine if the data were consistent and provide evidence that the otolith age estimates obtained in the current study are accurate.

Analysis of tag-recapture data from IOTTP

Further age validation for bigeye tuna was undertaken using the raw tag-recapture data from the IOTTP. Using the method described above, we estimated the age at recapture for all fish recaptured, not just the 15 selected for reading in the current study (i.e., by summing the estimated age of the fish when it was tagged/released and the time at liberty). Only fish <70 cm FL at release were included in the analysis to be confident in the estimated age at release. The length-at-age (estimated at recapture) was compared to the length-at-age estimated for

all fish aged in the study, to determine if the data were consistent providing further evidence that the annual ageing method is accurate.

2.4. Growth analysis

Three different growth models were fit to the age and length data for bigeye tuna: (1) von Bertalanffy (1938) (VB); (2) Richards (1959); and (3) von Bertalanffy with a logistic growth rate parameter (Laslett et al. 2002) (VB log k). Age estimates from both daily counts and annual counts after applying the decimal age algorithm were included in the models.

The VB growth model has the form:

$$L_a = L_\infty(1 - e^{-k(a-a_0)})$$

where L_a is the fork length at age a, L_∞ is the mean asymptotic length, k is a relative growth rate parameter (year^{-1}), and a_0 is the age at which fish have a theoretical length of zero. We fit the model using maximum likelihood estimation assuming a Gaussian error structure with mean 0 and variance σ^2.

The Richards model can be expressed in different ways, but here we used the following parameterisation:

$$L_a = L_\infty(1 - {}^1\!/_b\, e^{-k(a-a^*)})^b$$

where L_∞ and k are defined as for the VB model, a^* determines the point of inflection and b governs the shape of the curve. Note that when $b = 1$, the Richards equation is equivalent to the VB equation.

The VB log k model (Eveson et al. 2012; 2015) has the form:

$$L_a = L_\infty \left\{ 1 - e^{-k_2(a-a_0)} \left(\frac{1 + e^{-\beta(a-a_0-\alpha)}}{1 + e^{\alpha\beta}} \right)^{-\frac{(k_2-k_1)}{\beta}} \right\}$$

where this function allows for a change in growth from a VB curve with growth rate parameter k_1 to a VB curve with growth rate parameter k_2. There is a smooth transition between the two stages governed by a logistic function, where α governs the age at which the midpoint of the transition occurs and β governs the rate of the transition (being sharper for larger values).

To fit these models, we used maximum likelihood estimation assuming a Gaussian error structure with mean 0 and variance σ^2. Akaike's information criterion (AIC) (Akaike 1974) and plots of residuals were used to compare the fits.

3. Results

3.1. Daily ageing

Age estimates were obtained from all 39 otoliths selected for daily ageing. For 28 otoliths, the first two reads were within 10%, so the age estimate was the average of these two reads. For the remaining 11, a third read was required and the average of the closest two reads was taken. Age ranged from 49 to 509 days for the 37 small fish (18.5-79.0 cm FL) (Figure 4). Generally, the microincrement pattern along the preferred reading path (Figure 5) was relatively straight forward to interpret and consisted of clear opaque and translucent zones with few areas that required interpolation. However, it was observed that as the otoliths became larger, they became more difficult to age. This was mainly due to an increase in areas within the otolith, particularly closer to the outer edge, where the microincrements were more difficult to interpret due to splitting or merging of zones or the increasing presence of diffuse black otolith material. However, even in the largest otolith prepared for daily ageing, areas of clear-to-interpret microincrements could still be observed close to the margin (Figure 6).

The age estimates for the two larger fish (82.5 and 82.9 cm FL) were 603 and 822 days but due to the relative difficulty in ageing these samples compared to the smaller samples, and the fact that the difference in age was 219 days even though the fish were very similar in size, these two daily age estimates were not included in the growth analysis.

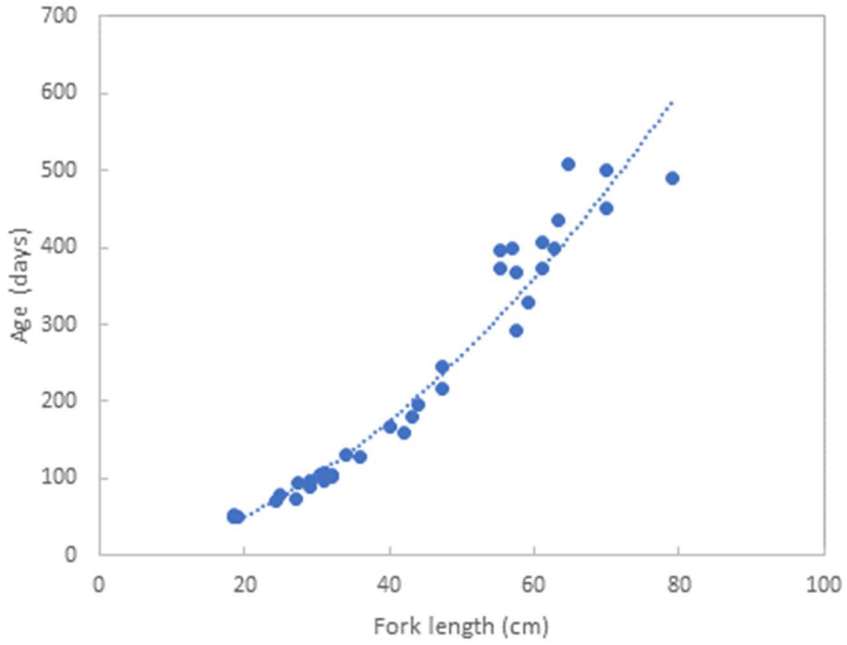

Figure 4. Relationship between fork length (cm) and daily age (microincrement count from longitudinal section) with fitted power curve for bigeye tuna for fish ≤79 cm. R^2 = 0.9763.

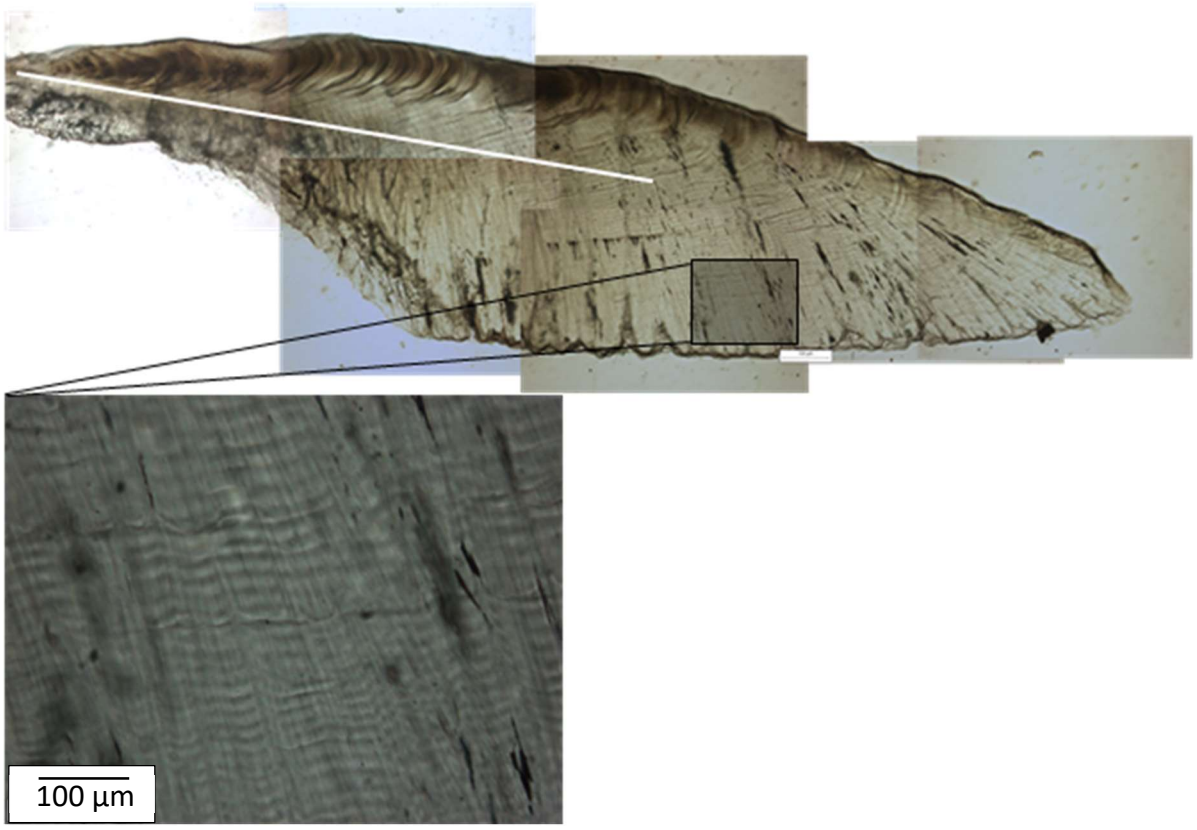

Figure 5. Image of a bigeye tuna otolith prepared as a longitudinal section for daily ageing. Fish of 30.5 cm FL with a total estimated age 105 days. The white line is the preferred counting path. Scale bar on both images is 100 µm.

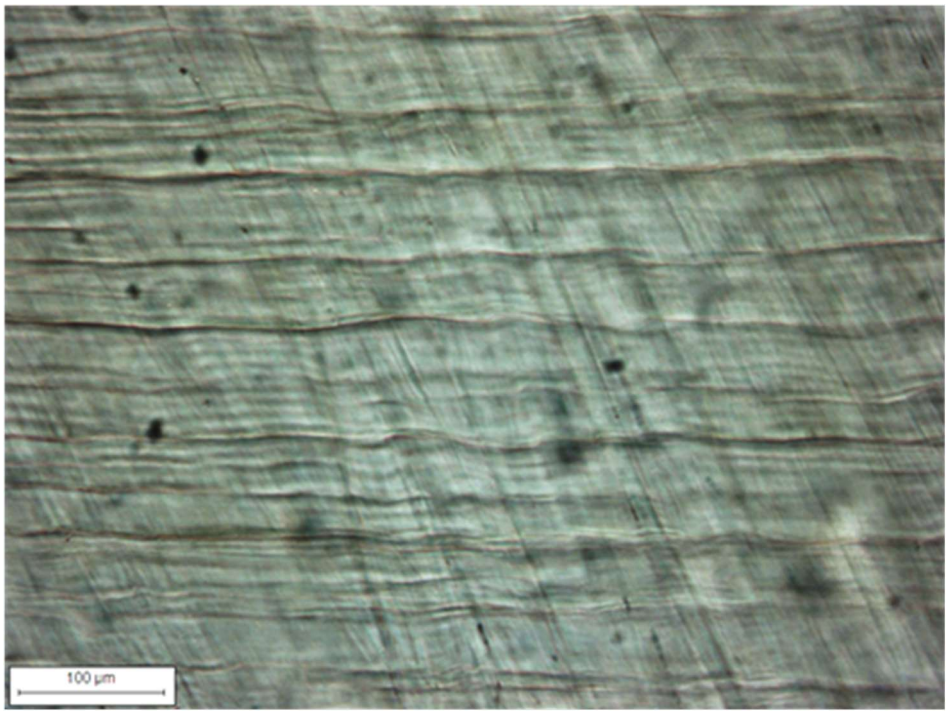

Figure 6. Image of the microincrement zone structure near the outer edge of one of the larger samples aged from counts of micro-increments. Fish of 69.9 cm FL with a total estimated age of 452 days.

Daily age estimates for the nine transverse sections re-read by FAS were lower than obtained by either Team 1 or Team 2 in the Sardenne et al. (2015) study (Figure 7). The FAS reader noted that interpreting the micro-structure was difficult and resulted in age estimates that were of low confidence. Differences in interpretation between readers could be due to two factors. First, readers in the Sardenne et al. (2015) may have been counting more zones in the initial part of the otolith. The prominent zones along the count path often consisted of a few smaller zones (see Figure 8). Along the initial count path that FAS use, the zone pattern is far more consistent and obvious. Secondly, the prepared sections were reasonably thick (approx. 120 µm) compared to the thickness that FAS prepare otoliths for transverse daily ageing (approx. 60 µm). The reason otoliths are polished to a thin level is to reduce the risk of counting the same increment more than once due to the curvature of the increments.

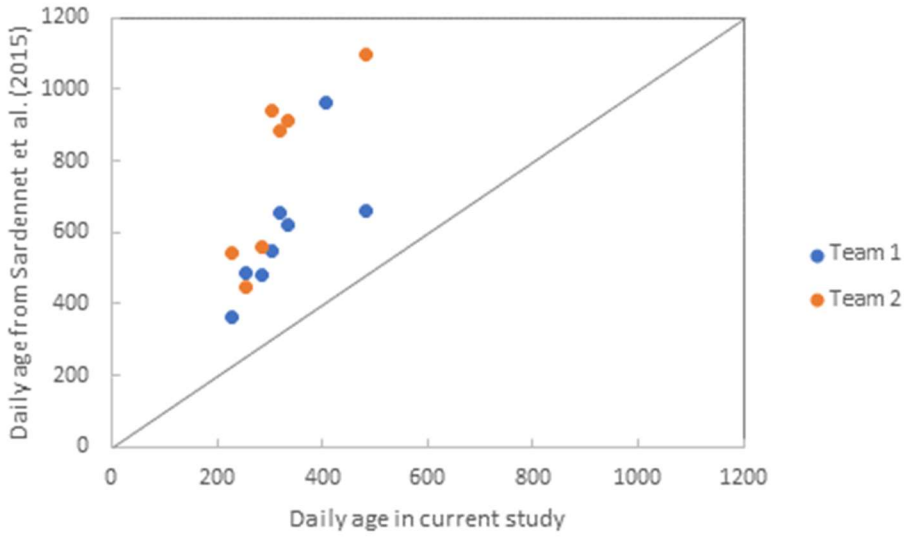

Figure 7. Comparison of daily age estimates by FAS in the current study and by Team 1 and 2 in Sardenne et al. (2015).

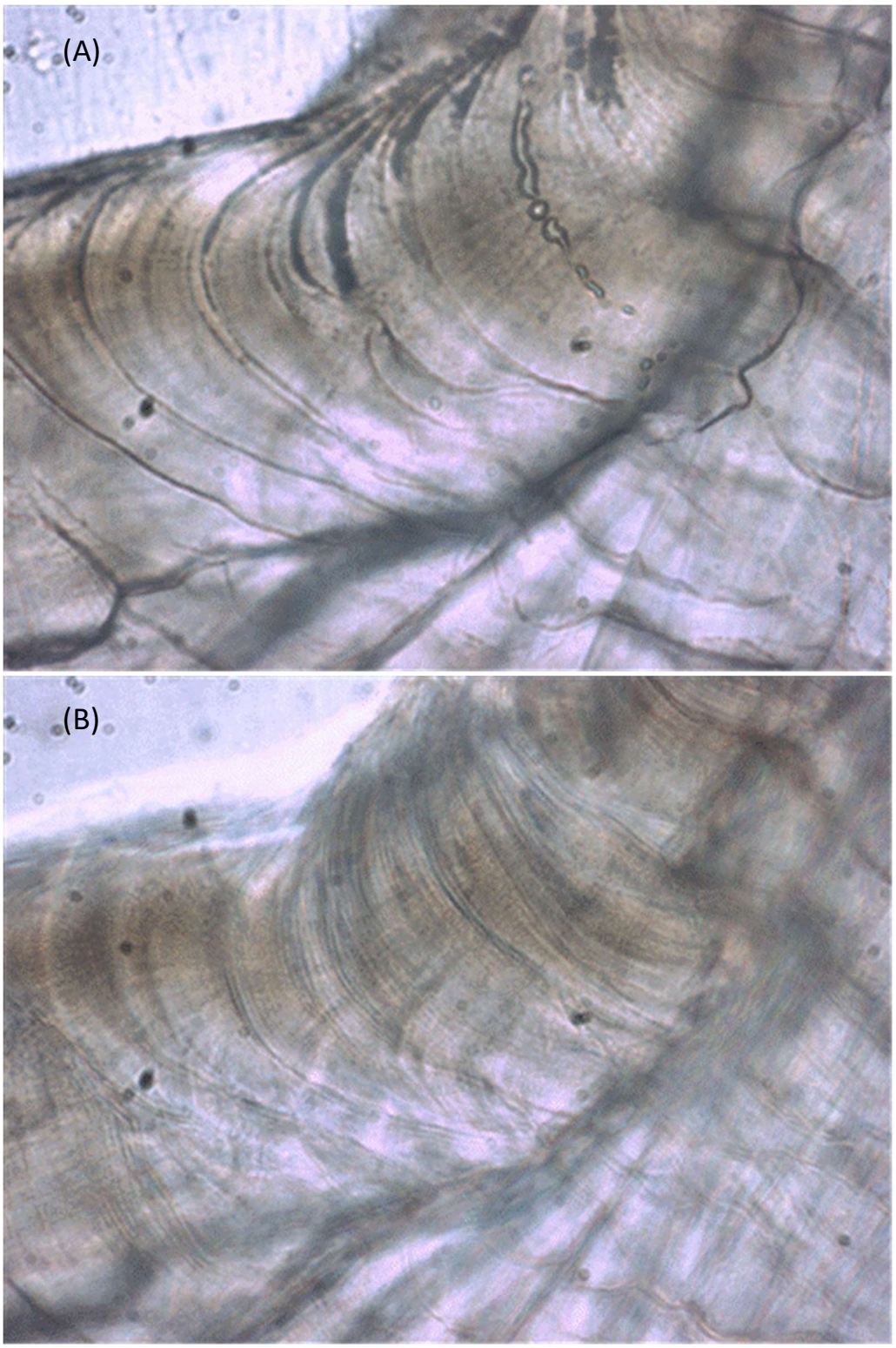

Figure 8. Two images of the same region within a transversely prepared otolith from Sardenne et al. (2015) magnified at 250x using two different focal distances. A) focus is on the surface (including the etched increments) and B) focus is on the increments under the surface.

3.2. Annual ageing

Counts of opaque zones were obtained for all 103 otoliths read for annual ageing. The counts ranged from 0 to 14 years. Figure 9 is an example of an otolith prepared for annual ageing with the (assumed) annual opaque zones marked. The inter-reader average percent error between readings was 3.4% with a maximum difference of 1 year (Table 1).

The relationship between fish length and otolith length on the counting path was linear (Figure 10), confirming that otoliths continue to growth throughout life and that increment widths are likely to be proportional to fish growth. Decimal age was calculated for each fish based on the algorithm described in section 2.2 "Annual ageing". The calculated decimal ages ranged from 0.13 to 14.7 years. Note that the age and otolith size of one fish did not correspond to the fork length and was removed from further analysis (8.04 years, 76.4 cm FL, see Figure 10) leaving 102 annual age estimates.

When daily and annual age estimates from the same fish were directly compared (n=32), the linear relationship was almost identical to the 1:1 line of agreement (Figure 11), indicating that the method to calculate decimal age from annual counts for these fish is working successfully. For fish with both a daily and annual age estimate, the daily estimate was included in the growth analysis. Thus, 70 annual age estimates were included in the growth models (103 total - 1 outlier - 32 daily estimates).

The relationship between otolith weight and age was curvilinear with a high goodness of fit (Figure 12), suggesting that otolith weight may be a good indicator of age, particularly for small/young fish.

Figure 9. Transverse preparation of a bigeye tuna otolith prepared for annual reading showing presumed annual opaque zones indicated by a white circle (n=11). Fish of length 148.2 cm FL.

Table 1. Difference in age estimates between otolith readings by Fish Ageing Services (FAS) and CSIRO for bigeye tuna.

Difference	Frequency	% Frequency
-2	1	0.97
-1	15	14.6
0	**72**	**69.9**
1	14	13.6
2	1	0.97
	103	100

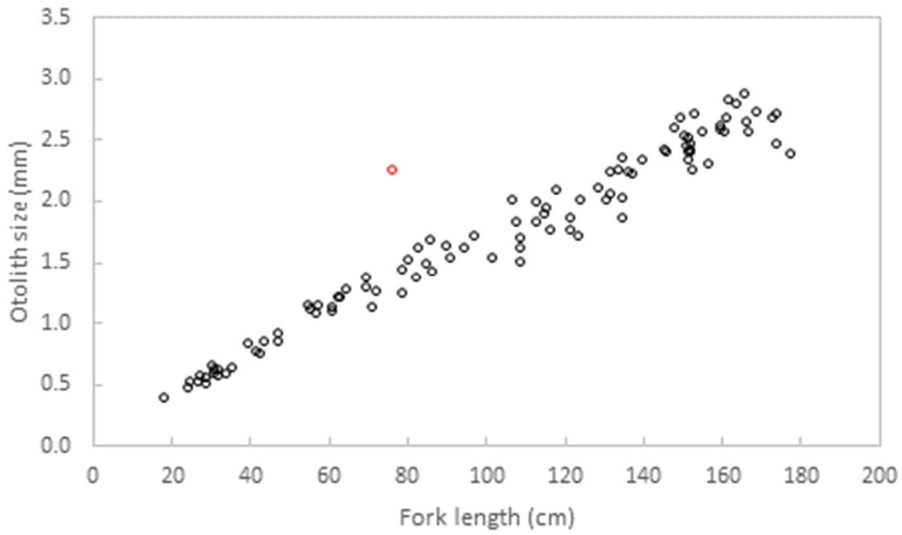

Figure 10. Relationship between fish length and otolith size (distance from the primordium along the counting path in transverse section) (n=103). One clear outlier (red point) was removed from the growth analysis.

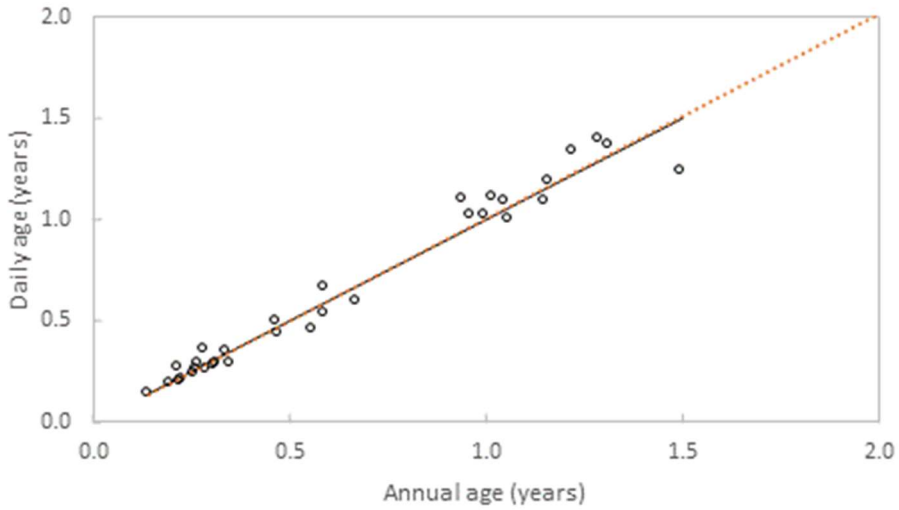

Figure 11. Comparison of daily and annual age estimates from sectioned otoliths sampled from the same fish (n=32). The 1:1 line is shown (solid black line) and the linear relationship between daily and annual age (dashed orange line; R^2 = 0.9681). Note that the daily age estimates from the two largest fish (82.5 and 82.9 cm FL) were not included in this comparison due to the low confidence in the age estimates.

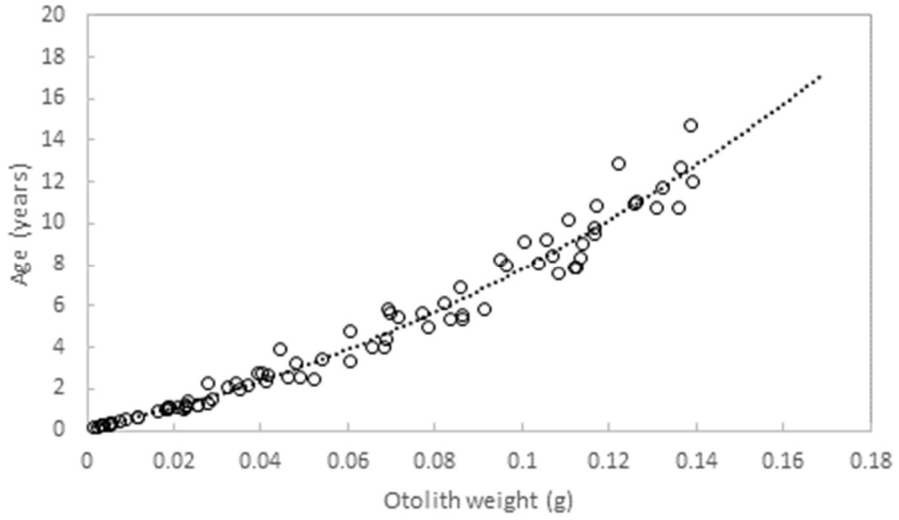

Figure 12. Relationship between otolith weight and estimated age (n=81).

3.3. Age validation and verification

Figure 13 shows the estimated age (daily and annual) of bigeye tuna obtained in the current study against otolith size (transverse section). The same information for bigeye tuna recaptured from the IOTTP, for which we have an otolith size estimate, is also shown in Figure 13; for these individuals age at recapture was estimated from length at release and time at liberty (see Methods). The consistency of the independent data sets for bigeye tuna <age 8 years suggests that the otolith age estimates are accurate. There is one outlier in the IOTTP

data (age 5), where the otolith is larger than expected for the calculated age; this could be due to the otolith not belonging to the tagged fish or incorrect tagging data (i.e., time at liberty). Additional work will be undertaken on the OTC marked otoliths to evaluate whether the number of increments after the OTC mark is consistent with the time at liberty.

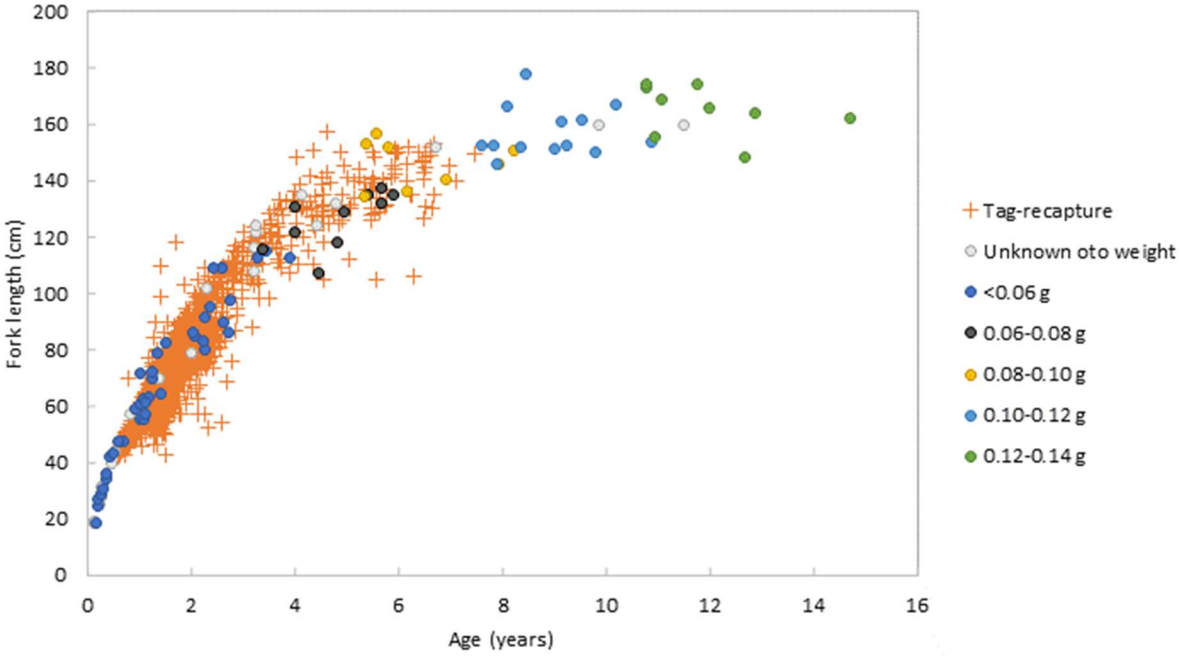

Figure 14 shows the length and age estimates for all bigeye tuna aged in the current study as well as for bigeye tuna recaptured in the IOTTP (in these cases age was estimated from release length and time at liberty). Again, the similarity of the independent data sets provides further evidence that the otolith ageing method used in this project is accurate. Unfortunately, the longest time at liberty for a tagged bigeye tuna was only 6.8 years, so this method can only verify age estimates up to ~8 years. However, the higher otolith age estimates obtained in the current study seem realistic since the otoliths were considerably heavier than the otoliths from fish aged 7-8 years (

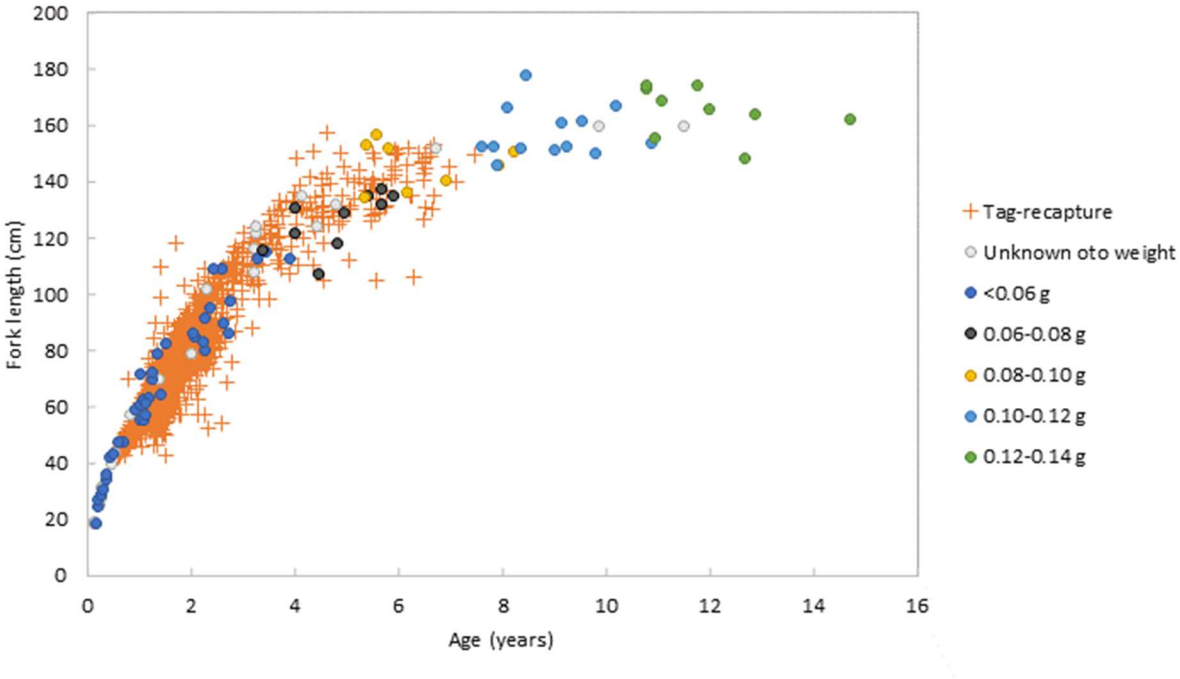

Figure 14).

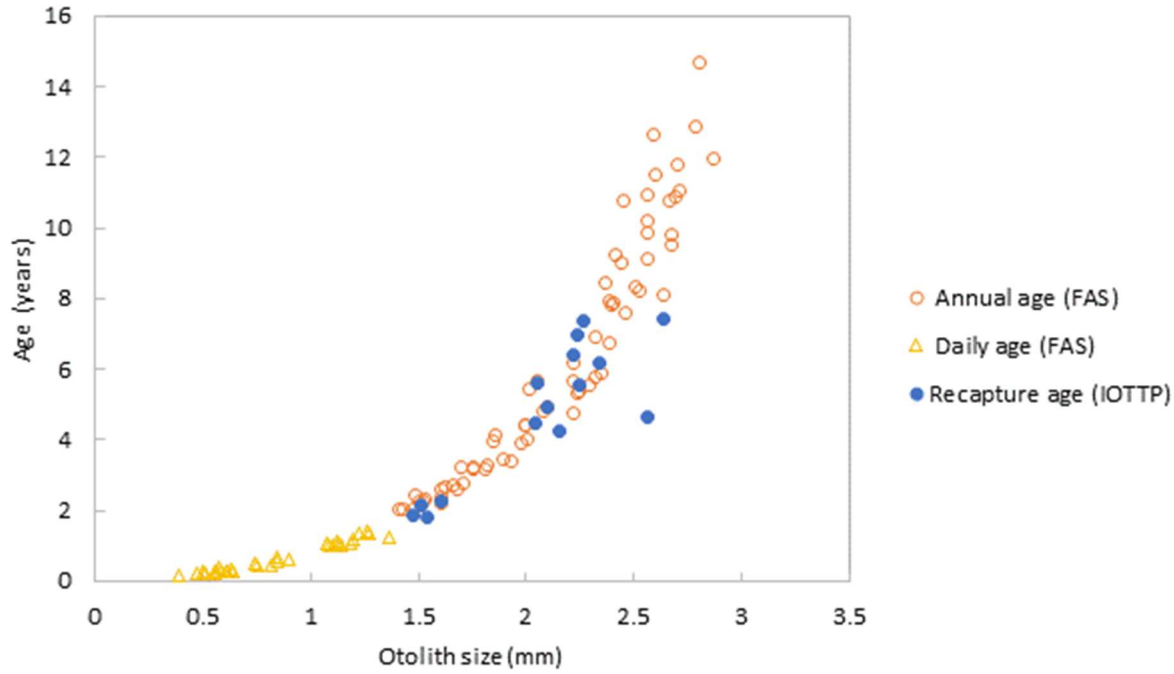

Figure 13. Otolith size versus age estimated by FAS (daily and annual) for bigeye tuna in this study as well as otolith size versus estimated recapture age of bigeye tuna that were tagged and recaptured in the IOTTP and for which otolith size was measured in the current study (n=15). Recapture age was estimated from release length and time at liberty (see Methods section 2.3). Otolith size is the distance from the primordium to the edge in transverse sectioned otoliths.

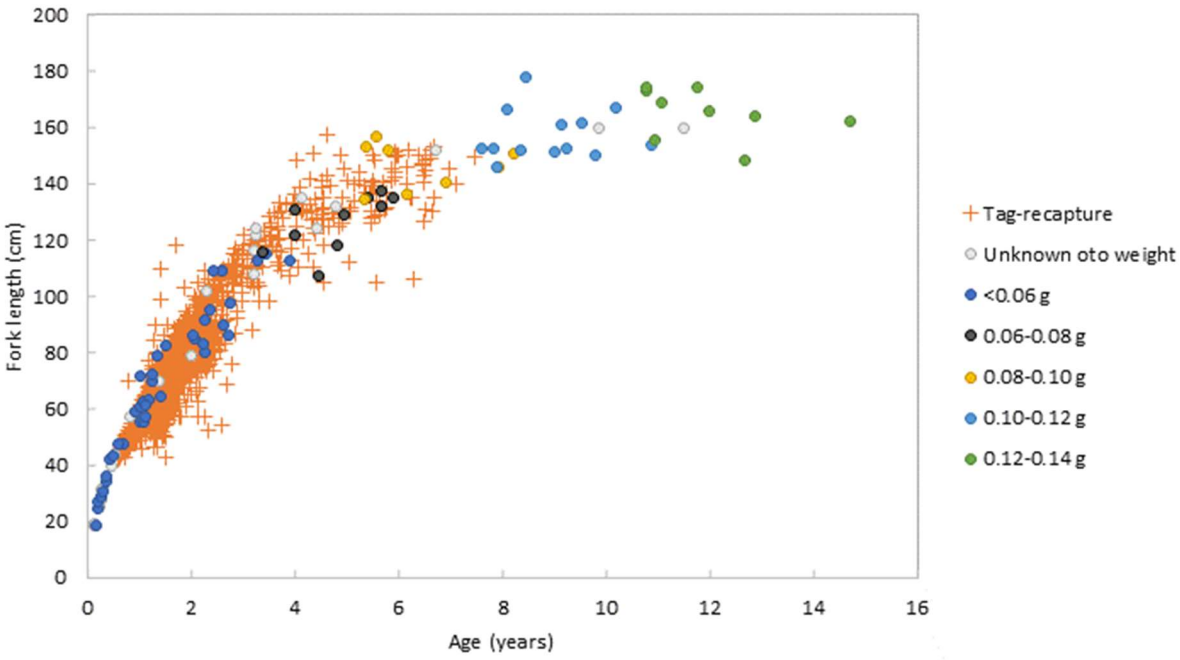

Figure 14. Age versus length data obtained in the current study shown by otolith weight bin (see key; g = grams). Also shown is age versus length at recapture for bigeye tuna tagged and recaptured in the IOTTP. Recapture age was estimated from release length and time at liberty (see Methods section 2.3).

3.4. Growth analysis

A total of 107 age-length data points were included in the growth models (70 decimal annual age estimates and 37 daily age estimates). The three growth models (VB, Richards and VB log k) provide very similar fits to the data (Figure 15; Append Figure 3). The AIC values are also very similar, with the lowest value for the Richards model being within 1.5 units of the largest value for the VB log k model (Table 2). Based on residuals, the two-phase VB log k model provides the best fit to the smallest fish (<40 cm FL) (Figure 15B; Append Figure 3). The VB log k model indicates a transition between two growth phases, from fast growth up to ~40 cm FL, followed by slower growth before increasing again. This can be described by two phases of VB growth, with a high growth rate parameter in the first phase (k_1=0.68) followed by a lower growth rate parameter in the second phase (k_2=0.29) (Table 2).

Since otolith weight may be an indicator of age, we examined the otolith weight to fish length relationship of a larger number of samples (n=332) than were aged (n=107), to ascertain if the otolith growth was consistent with the observed fish growth. The results show a similar pattern in growth, with a transition at ~40 cm FL from fast growth to slower growth before increasing again, lending support to the VB log k model (Figure 16). These transitions in otolith growth (and presumably fish growth) were not observed in bigeye tuna otoliths from the WCPO (Figure 16), suggesting slightly different growth patterns for juvenile bigeye tuna between these oceans. However, overall, bigeye tuna growth in the Indian Ocean and Western Pacific Ocean appears to be similar.

The length-at-age data were insufficient to model sex-specific or region-specific growth within the Indian Ocean. However, preliminary data exploration indicated that males may

grow slightly faster and reach slightly larger sizes, on average, than females (Append Figure 4). This was supported by the length-at-otolith weight data for a larger number of samples (Append Figure 5). There is some indication in the length-at-age data that bigeye tuna in the western Indian Ocean may grow slightly slower than bigeye tuna in the eastern Indian Ocean (Append Figure 6), but the sample size is too small to be conclusive and other factors such as size-selective fishing could bias the data. The length-at-otolith weight data were also consistent with this result but very few samples were available from the eastern Indian Ocean in the current project (Append Figure 7). Additional data were obtained for bigeye tuna from an earlier study in the eastern Indian Ocean (Farley et al. 2006; all were >70 cm FL), which did not indicate the presence of a difference in otolith growth (and presumably fish growth) between the western and eastern Indian Ocean (Append Figure 7).

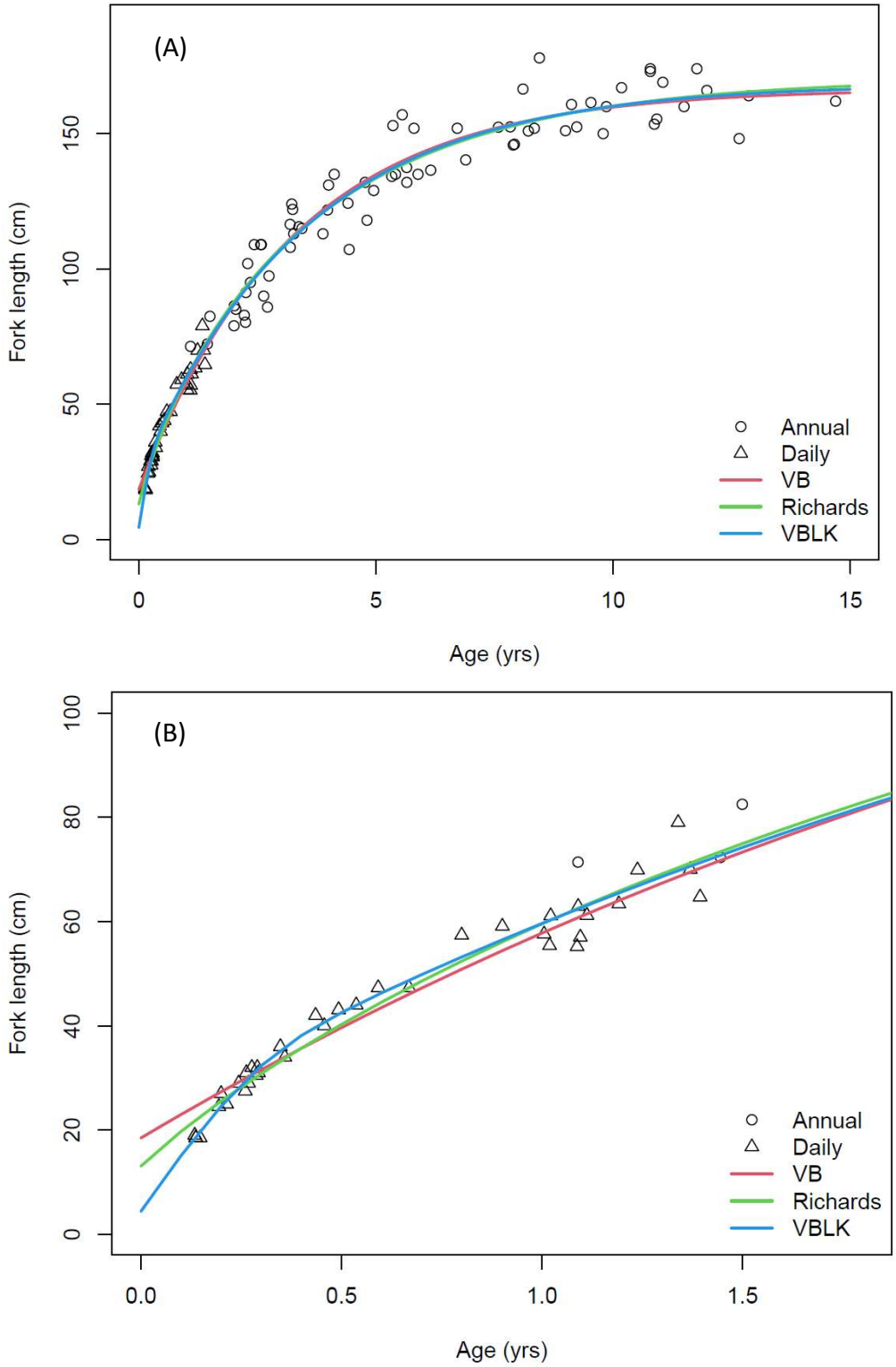

Figure 15. (A) Length-at-age data (daily and annual) for bigeye tuna with von Bertalanffy (VB), Richards and von Bertalanffy log k (VBLK) growth models fit to the data. (B) A close-up of the length-at-age data and growth curves shown in (A) for small/young bigeye tuna.

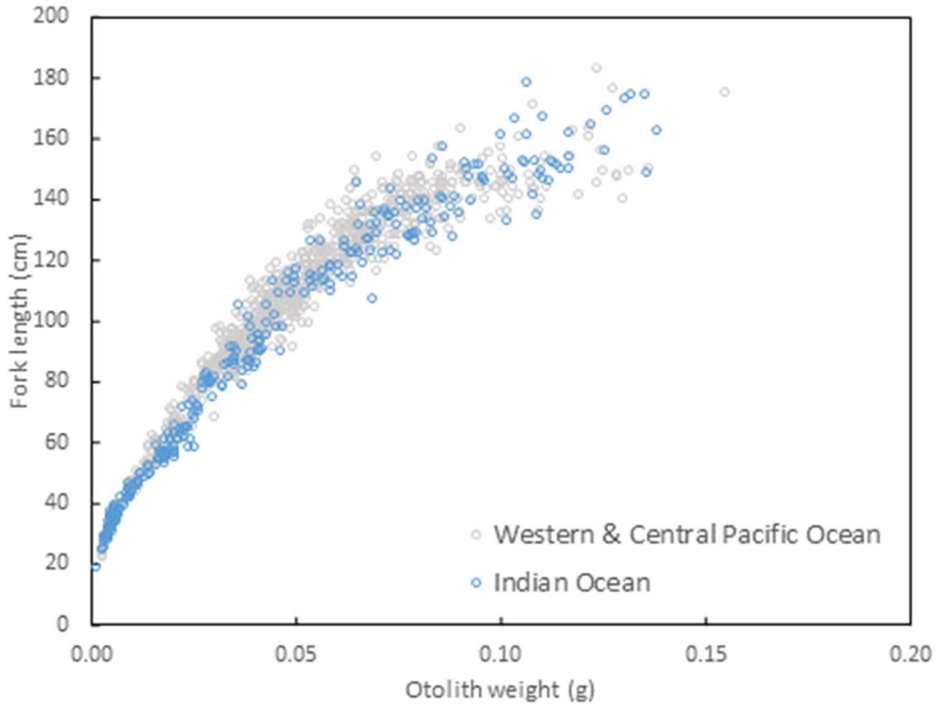

Figure 16. Relationship between otolith weight and fork length for bigeye tuna in the Indian Ocean from the current study (i.e., GERUNDIO, EMOTION, PSTBS_IO and IOTTP projects) (n=332) and in the western and central Pacific Ocean from Farley et al. (2019; 2020) (n=806; 12 outliers were removed).

Table 2. Parameter estimates from fitting von Bertalanffy (VB), Richards and VB log k growth models to the bigeye tuna length at age data (n=107). Standard errors for the parameter estimates are given in parentheses.

Model	L_∞	k/k_1	k_2	α	b/β	a_0/a^*	σ	AIC
VB	166.6 (2.2)	0.31 (0.01)	--	--	--	-0.38 (0.05)	7.44 (0.51)	741.0
Richards	170.5 (3.7)	0.25 (0.03)	--	--	0.75 (0.10)	-1.29 (0.61)	7.34 (0.50)	740.3
VB log k	168.3 (2.5)	0.69 (1.4)	0.29 (0.02)	0.35 (1.0)	13.1 (49.3)	-0.04 (0.29)	7.26 (0.50)	741.8

4. Discussion

Otoliths are the preferred calcified structure to estimate fish age as they permanently record patterns in growth over time. Age estimates from counts of microincrements are generally limited to young/small fish (Campana 1992; Williams et al. 2012) and the otoliths must be examined under high magnification. Sub-daily increments and discontinuities may also be present, and the daily deposition of increments appears to cease in juvenile and/or adults of long-lived species, including tunas (Wright et al. 2002; Williams et al. 2012). Validated counts of annuli in otoliths, however, have been widely used to obtain estimates of age of tuna species, including bigeye tuna. The recent methods developed by Farley et al. (2020) to estimate a decimal age for bigeye and yellowfin tuna in the WCPO, based on a combination

of validated daily and annual age estimates, provide a more precise estimated growth curve for the species, and have now been applied to other species including yellowfin tuna, albacore tuna (*Thunnus alalunga)* and striped marlin (*Kajikia audax*) (Farley et al. 2020, 2021a, b).

For bigeye tuna in the Indian Ocean, Stéquert and Conand (2004) recommended that a scanning electronic microscope (SEM) should be used to estimate the age of bigeye tuna >120 cm FL due to the small size of the microincrements in otoliths. Sardenne et al. (2015) also found that daily age estimates for bigeye tuna >100 cm FL were underestimated using a standard light microscope. In the current study, estimates of daily age were limited to fish <80 cm FL due to the difficulty interpreting the sub-structure and discontinuities in otoliths of larger fish. The daily age data aligned well with the annual age data for small/young fish (see Figure 15), supporting our method to calculate the decimal age of bigeye tuna. The preliminary age validation/verification work using otoliths and data from the IOTTP provides evidence that the otolith ageing method used in this study is accurate. However, we recommend that further age validation work is undertaken.

The two-phase VB log k model provided a better fit to the length at age data for fish <40 cm FL than the other models. The length-at-otolith weight data (which is independent of the age estimation method) also showed a change in otolith growth at ~40 cm FL consistent with the length-at-age data, which lends support for the VB log k growth model. Overall, our analysis shows that growth is rapid in the first few years with fish reaching ~60 cm FL at age 1 and ~85 cm FL at age 2. Mean asymptotic length was estimated to be ~168 cm FL and maximum age is at least 14 years.

Our VB log k growth curve for bigeye tuna is similar to the VB curve of Stéquert and Conand (2004) for bigeye tuna in the western Indian Ocean, which was estimated using counts of microincrements (daily age estimates) in otoliths (Figure 17). A difference occurred for fish <~40 cm FL, where our data suggests slightly faster growth rates. The raw length-at-age data for fish >40 cm are very similar between the two studies, although we obtained higher age estimates for fish >140 cm FL. This is most likely due to microincrements no longer forming daily marks in the otoliths of large/old fish, but since this occurred after growth slowed and around their asymptotic length, the growth curves obtained were similar.

Although our data suggest two-phase growth for bigeye tuna, the VB log k growth curve we estimated is quite different from the VB log k curves of Eveson et al. (2015), which were based on tag-recapture data from the IOTTP and otolith-based daily age estimates from Sardenne et al. (2015) (Figure 17). The tagging data were most influential in determining the shape of the growth curves in Eveson et al. (2015); however, the otolith ageing data were useful for estimating the age of the tagged fish at release. Daily age data were available from three otolith reading teams in Sardenne et al. (2015), and although the daily increment deposition rate was validated for bigeye tuna (note each team had a reading bias linear model developed to convert microincrement counts to a daily age estimates), the age estimates still varied considerably between Team 1 and Teams 2 and 3, and also between FAS and Teams 1 and 2 for the nine otoliths re-read in this study, which highlights that otolith structure can be interpreted differently by different readers. Eveson et al. (2015) estimated three growth curves, all using the same tag-recapture data but using daily age data from each reader team

separately; this resulted in a shift of the curve along the age axis depending on which team's data were used. All three growth curves showed a two-stanza growth pattern with very slow growth for fish between 40 and 50 cm FL, then faster growth between 50 and 70 cm FL, before slowing again. The lack of age data for fish <40 cm FL meant the shape of the early part of the growth curve was uncertain for all teams (Eveson et al. 2015).

The daily age estimates and growth curve obtained in the current study are more similar to the Eveson et al. (2015) "Team 1" growth curve than the "Team 2" curve that was used in the 2019 stock assessment. This is due to the similar length-at-daily age estimates obtained in the current study and Team 1 compared to Teams 2 and 3 (Append Figure 8). However, our growth curve does not show the same very slow growth for fish <50 cm FL (Figure 17). In addition, our growth curve has a higher mean asymptotic length (~168 cm FL) compared to Eveson et al. (2015) (152.5 cm FL for all three curves). This may be due to the low number of fish >150 cm FL in the tag-recapture data available at the time for use in Eveson et al. (2015), which is likely related to the relatively short times at liberty of fish included in the analysis (<6 years) compared to the estimated longevity of bigeye tuna of at least 14 years.

There has been discussion about whether the two-stanza growth pattern obtained for bigeye tuna in the Indian Ocean from analysis of tagging data is a true reflection of growth of the population (Kolody 2011; Maunder et al. 2015). Two-stanza growth patterns have been detected in the data of some bigeye tuna tagging studies in the western and central Pacific Ocean (WCPO) and the eastern Atlantic Ocean (Lehodey et al. 1999; Gaertner et al. 2009) but not in other studies (Hallier et al. 2005; Cayré and Diouf 1984), and it has not been reported in studies that only used otolith age data (see review by Murua et al. 2017). The reason for different growth curves reported amongst studies is unclear but could be due to a number of factors including environmental or genetic factors, selectivity of fishing gear or tagging effects (Kolody 2011; Maunder et al. 2015).

We recommend that additional otoliths are collected from the eastern Indian Ocean, and that these otoliths and additional otoliths from those already collected in the GERUNDIO and IOTTP projects are read/aged to provide further information on growth and longevity before the next stock assessment for bigeye tuna in 2022.

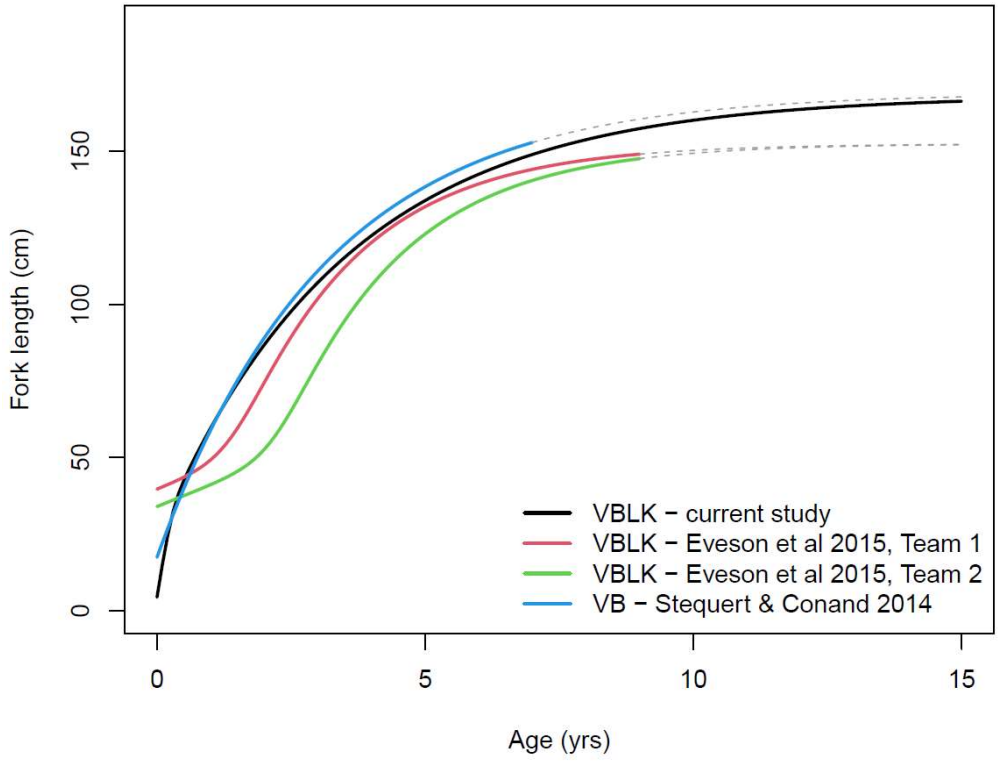

Figure 17. Comparison of the VB log k growth curve estimated in the current study with growth curves estimated for Indian Ocean bigeye tuna from other studies. The curves from Eveson et al. (2015) were based on tag-recapture data from the IOTTP and otolith daily age estimates from different reader teams (see Sardenne et al. 2015). The curve from Stéquert and Conand (2014) was based on otolith daily age data estimated using light microscopes and scanning electron microscopes. The solid, coloured section of each curve represents the range of the data from it was estimated. VB = von Bertalanffy, VBLK = VB log k.

Acknowledgements

We are grateful to the many vessel skippers and crew involved in the project. We gratefully acknowledge all the observers, port samplers and coordinators for collecting, storing and transporting otoliths across the Indian Ocean. We want to thank Iñigo Krug and Iñigo Onandia (AZTI) who assisted in fish sampling and otolith extraction of those individuals collected from the Spanish cannery. We also thank Admir Sutrovic, Graham Porter and Christine Rees (FAS) for preparing and or weighing the otoliths. We thank the EMOTION (ANR 11 JSV7 007 01) and PSTBS-IO (GCP/INT/233/EC) projects for permitting the use of otoliths and data collected during the projects. The tuna tagging data analyzed in this study were collected through the Indian Ocean Tuna Tagging Program (IOTTP) under the Regional Tuna Tagging Project of the Indian Ocean funded by the 9th European Development Fund (9.ACP.RSA.005/006) of the European Union, and small-scale tagging projects funded by the European Union and the Government of Japan, such as the West Sumatra Tuna Tagging Project. We wish to acknowledge the contributions of all the people that have been involved in the IOTTP and a

special thanks to Fany Sardenne and Julien Barde (IRD) who kindly assisted with the transport of otoliths to CSIRO. The project is supported by financial assistance of the European Union (contract no. 2020/SEY/FIDTD/IOTC - CPA 345335). The views expressed herein can in no way be taken to reflect the official opinion of the European Union.

References

Anon (2002). A Manual for Age Determination of Southern Bluefin *Thunnus maccoyii*. Otolith Sampling, Preparation and Interpretation. Available at: http://www.ccsbt.org/userfiles/file/docs_english/meetings/meeting_reports/ccsbt_09/report_of_daews.pdf/

Appleyard, S.A., Ward, R.D. and Grewe, P.M. 2002. Genetic stock structure of bigeye tuna in the Indian Ocean using mitochondrial DNA and microsatellites. Journal of Fish Biology 60: 767-770.

Beamish, R.J. and Fournier, D.A. (1981). A method for comparing the precision of a set of age determinations. Canadian Journal of Fisheries and Aquatic Sciences 38: 982–983. doi: 10.1139/f81-132.

Bodin, N., Chassot, M., Sardenne, F., Zudaire, I., Grande, M., Dhurmeea, Z., Murua, H., Barde, J. (2018). Ecological data for western Indian Ocean tuna. Ecology 99 (5) 1245-1245.

Campana, S.E. (1992). Measurement and interpretation of the microstructure of fish otoliths. In Otolith Microstructure Examination and Analysis'. Ed. by D. K. Stevenson, and S. E. Campana. Canadian Special Publication of Fisheries and Aquatic Sciences 117: 59–71.

Cayré, P., Diouf, T. (1984). Croissance du thon obèse (Thunnus obesus) de l'Atlantique d'apres les resultats de marquage. Madrid, International Commission for the Conservation of Atlantic Tunas (ICCAT). Rec.Doc. Sci. 20(1), 180-187.

Chiang, H-C, Hsu, C-C, Wu, GC-C, Chang, S-K and Yang, H-Y (2008). Population structure of bigeye tuna (*Thunnus obesus*) in the Indian Ocean inferred from mitochondrial DNA. Fisheries Research, 90: 305–312.

Collette, B.B., Boustany, A., Fox, W., Graves, J., Juan Jorda, M. & Restrepo, V. (2021). *Thunnus obesus*. The IUCN Red List of Threatened Species 2021: e.T21859A46912402. https://dx.doi.org/10.2305/IUCN.UK.2021-2.RLTS.T21859A46912402.en

Davies, C., Marsac, F., Murua, H., Fahmi, Z., Fraile, I. (2020). Summary of population structure of IOTC species from PSTBS-IO project and recommended priorities for future work. IOTC-2020-SC23-11_Rev1, 16p.

Díaz-Arce, N., Grewe, P., Krug, I Artetxe, I., Ruiz, J., et al. (2020). Evidence of connectivity of bigeye tuna (*Thunnus obesus*) throughout the Indian Ocean inferred from genome-wide genetic markers. IOTC-2020-WPTT22(AS)-16.

Eveson, P., Million, J., Sardenne, F., Le Croizier, G. (2012). Updated growth estimates for skipjack, yellowfin and bigeye tuna in the Indian Ocean using the most recent tag-recapture and otolith data. IOTC-2012-WPTT14-23.

Eveson, P., Million, J., Sardenne, F., Le Croizier, G. (2015). Estimating growth of tropical tunas in the Indian Ocean using tag-recapture data and otolith-based age estimates. Fisheries Research 163: 58–68.

Farley, J. H., Clear, N. P., Leroy, B., Davis, T. L. O., McPherson, G. (2006). Age, growth and preliminary estimates of maturity of bigeye tuna, *Thunnus obesus*, in the Australian region. Marine and Freshwater Research, 57: 713–724.

Farley, J., Eveson, P., Krusic-Golub, K., Kopf, K. (2021a). Southwest Pacific Striped Marlin Population Biology (Project 99). WCPFC-SC17-2021/SA-IP-11.

Farley, J., Eveson, P., Krusic-Golub, K., Sanchez, C., Roupsard, F., McKechnie, S., Nicol, S., Leroy, B., Smith, N., Chang, S.-K. (2017). Project 35: Age, growth and maturity of bigeye tuna in the western and central Pacific Ocean. WCPFC-SC13-2017/ SA-WP-01.

Farley, J., Krusic-Golub, K., Eveson, P. (2021b). Updating age and growth parameters for South Pacific albacore (Project 106). WCPFC-SC17-2021/SA-IP-10.

Farley, J., Krusic-Golub, K., Eveson, P., Clear, N., Rouspard, F., Sanchez, C., Nicol, S., and Hampton, J. (2020). Age and growth of yellowfin and bigeye tuna in the western and central Pacific Ocean from otoliths. WCPFC-SC16-2020/SC16-SA-WP-02.

Fu, D. (2019). Preliminary Indian Ocean bigeye stock assessment 1950-2018 (Stock Synthesis). IOTC–2019–WPTT21–61.

Gaertner, D., Hallier, J.P. (2009). An updated analysis of tag-shedding by tropical tunas in the Indian Ocean. IOTC-2009-WPTT-34.

Hallier, J.P., Stéquert, B., Maury, O., and Bard, F.-X. (2005). Growth of bigeye tuna (*Thunnus obesus*) in the eastern Atlantic Ocean from tagging-recapture data and otolith readings. Col. Vol. Pap. ICCAT 57: 181–194.

IOTC (2020). Report of the 22nd Session of the IOTC Working Party on Tropical Tunas, Stock Assessment Meeting. OTC–2020–WPTT22(AS)–R[E]_Rev1.

Kolody, D. (2011). Can length-based selectivity explain the two stage growth curve observed in Indian Ocean YFT and BET? OTC–2011–WPTT13–33.

Laslett, G.M., Eveson, J.P., Polacheck, T. (2002). A flexible maximum likelihood approach for fitting growth curves to tag-recapture data. Can. J. Fish. Aquat. Sci. 59, 976–986.

Lehodey, P., Leroy, B. (1999) Age and growth of yellowfin tuna (*Thunnus albacares*) from the western and central Pacific Ocean as indicated by daily growth increments and tagging data. Working paper YFT-2, 12th meeting of the Standing Committee on Tuna and Billfish, Tahiti.

Maunder, M.N., Crone, P.R., Valero, J.L., Semmens, B.X. (2015). Growth: theory, estimation, and application in fishery stock assessment models CAPAM Workshop Series Report 2 March 2015.

Murua, H., Eveson, J.P., Marsac, F. (2015). The Indian Ocean Tuna Tagging Programme: Building better science for more sustainability. Fish. Res. 163:1-6.

Murua, H., Rodrıguez-Marin, E., Neilson, J., Farley, J., Juan-Jorda, M.J. (2017) Fast versus slow growing tuna species – age, growth, and implications for population dynamics and fisheries management. Rev. Fish Biol. 27: 733-773. DOI 10.1007/s11160-017-9474-1

R Core Team (2021). R: A language and environment for statistical computing. R Foundation for Statistical Computing, Vienna, Austria. URL https://www.R-project.org/.

Richards, F.J. (1959). A flexible growth function for empirical use. J. Exp. Bot. 10(2): 290-301.

Sardenne, F., Dortel, E., Le Croizier, G., Million, J., Labonne, M., Leroy, B., Bodin, N., Chassot, E. (2015) Determining the age of tropical tunas in the Indian Ocean from otolith microstructures. Fish. Res. 163:44–57. doi:10.1016/j.fishres.2014.03.008

Stéquert, B., Conand, F. 2004. Age and growth of bigeye (*Thunnus obesus*) in the western Indian Ocean. Cybium 28(2): 163-170.

von bertalanffy, L (1938). A quantitative theory of organic growth (inquiries on growth laws. II). Human Biol 10: 181–213.

Williams AJ, Farley JH, Hoyle SD, Davies CR, Nicol SJ (2012) Spatial and sex-specific variation in growth of albacore tuna (*Thunnus alalonga*) across the South Pacific Ocean. PLoS ONE 7(6): e39318. doi:10.1371/journal.pone.0039318.

Williams, A.J., Leroy, B.M., Nicol, S.J., Farley, J.H., Clear, N.P., Krusic-Golub, K., Davies, C.R, (2013) Comparison of daily- and annual- increment counts in otoliths of bigeye (*Thunnus obesus*), yellowfin (*T. albacares*), southern bluefin (*T. maccoyii*) and albacore (*T. alalunga*) tuna. ICES J. Mar Sci 70(7): 1439–1450. doi:10.1093/icesjms/fst093.

Wright, P.J., Panfili, J., Morales-Nin, B., Geffen, A.J. (2002). Types of calcified structures. In: Manual of fish Sclerochronology. (Eds J Panfili, HD Pontual, H Troadec, PJ Wright.) pp. 31–57. (Ifremer-IRD coedition: Brest, France).

Appendix A – Otolith data for age algorithm

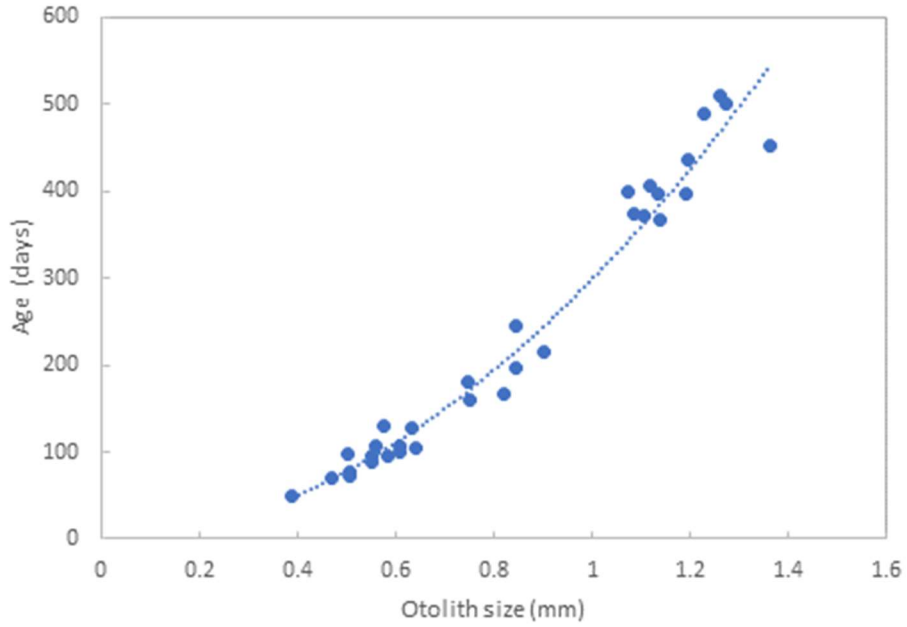

Append Figure 1. Relationship between daily age and otolith size with fitted power curve for bigeye tuna. Otolith size is the distance from the primordium to the edge in transverse sectioned otoliths. R^2=0.9765.

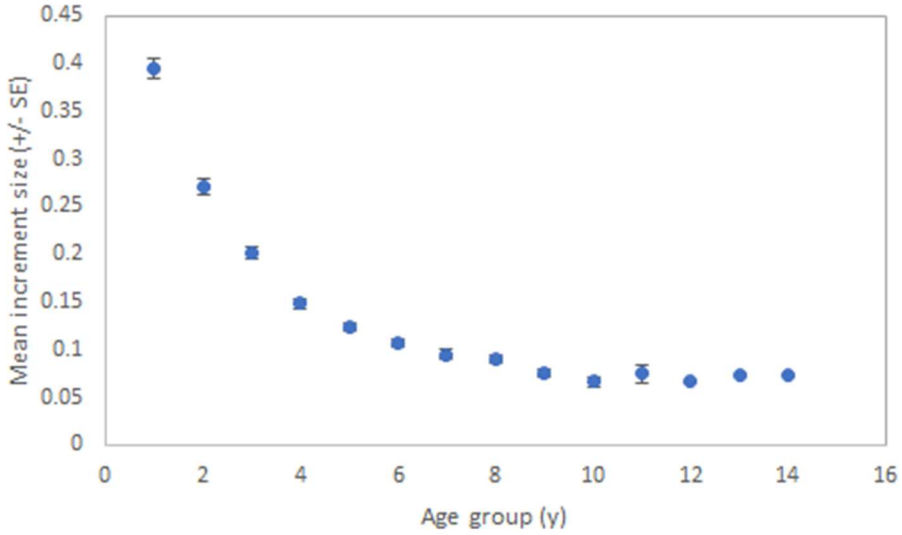

Append Figure 2. Mean (+/- SE) annual increment width in millimetres by age class for bigeye tuna.

Appendix B – Diagnostic residual plots

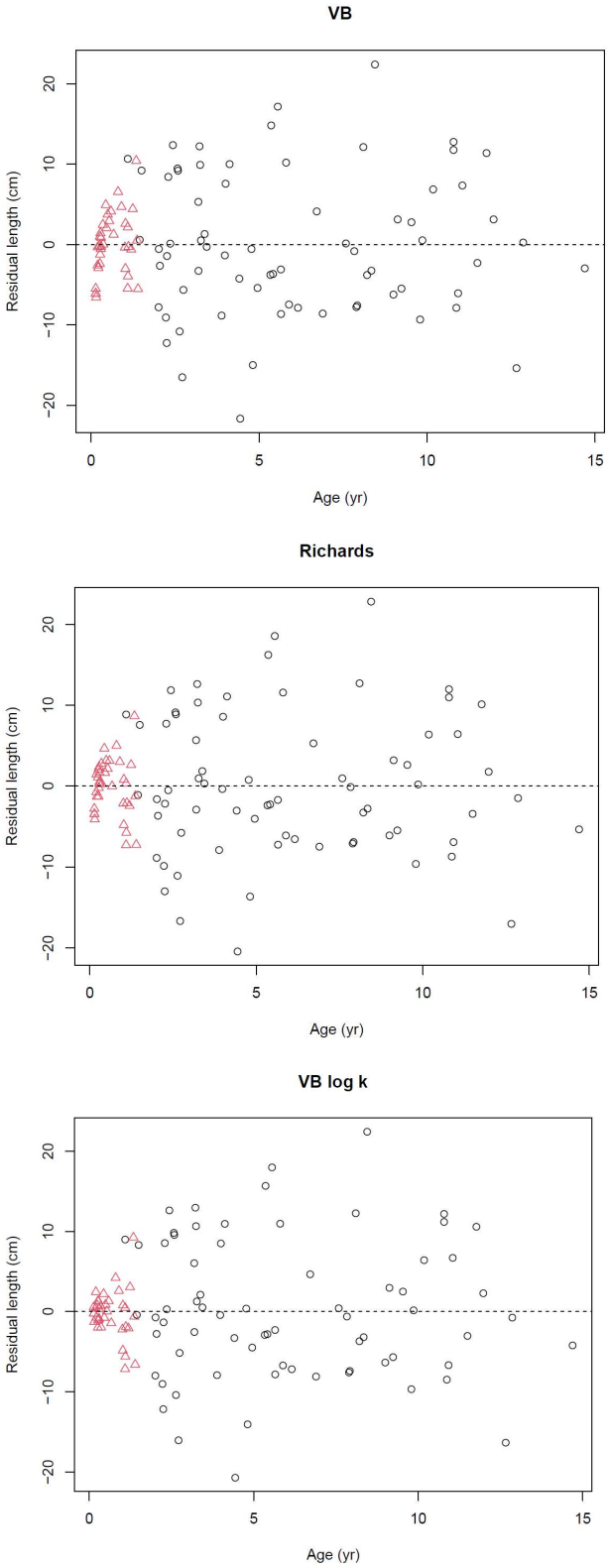

Append Figure 3. Diagnostic residual plots for the fit of the VB, Richards and VB log k growth models to the length at age data.

Appendix C – Growth by sex and region

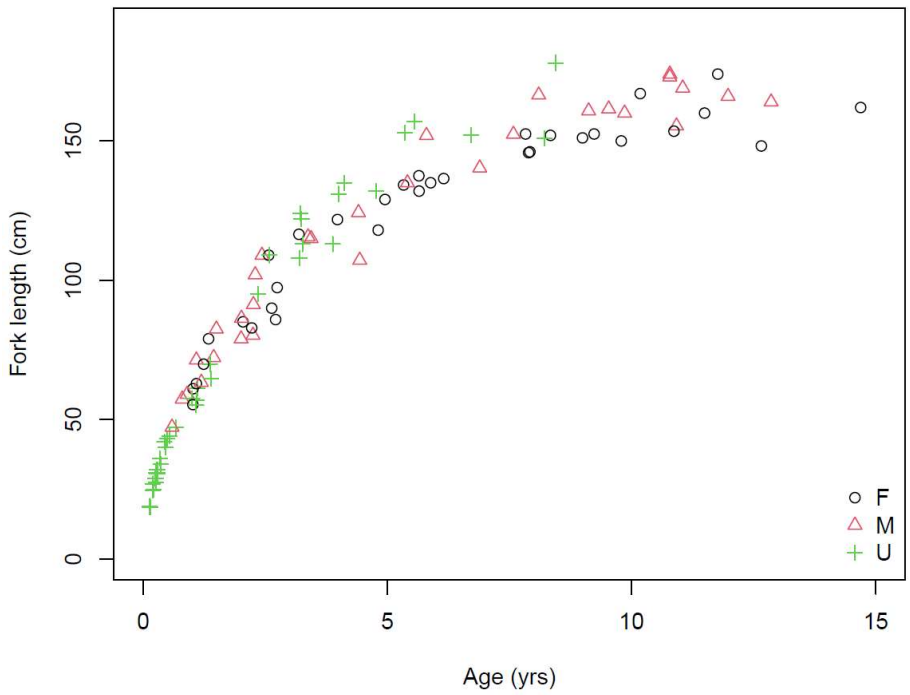

Append Figure 4. Length-at-age data for bigeye tuna in the Indian Ocean by sex. There is some indication that males may grow slightly faster and reach slightly larger sizes, on average, than females.

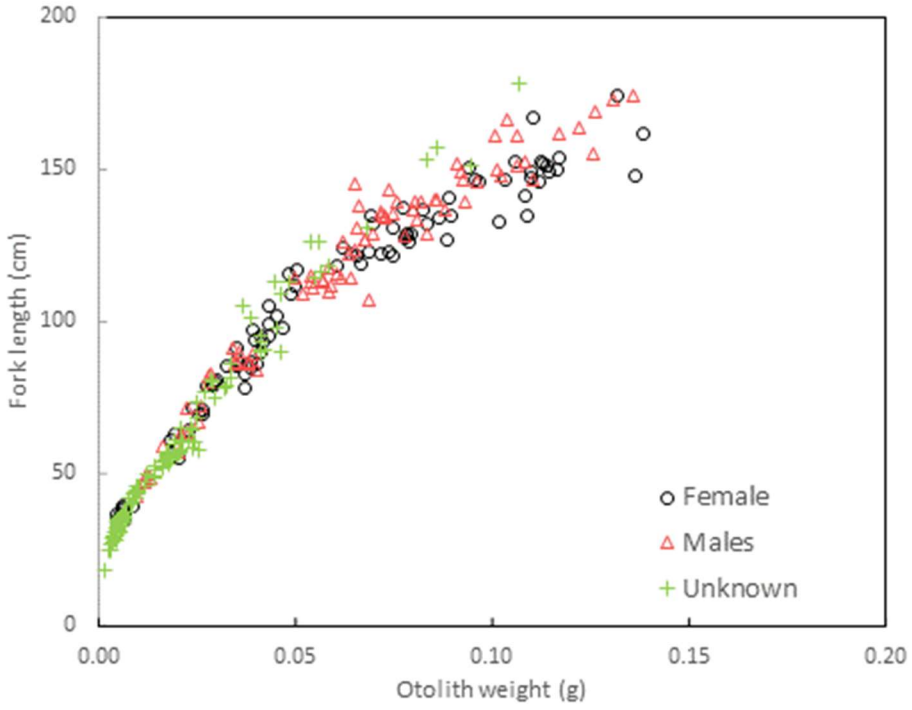

Append Figure 5. Relationship between otolith weight and fork length for bigeye tuna in the Indian Ocean by sex.

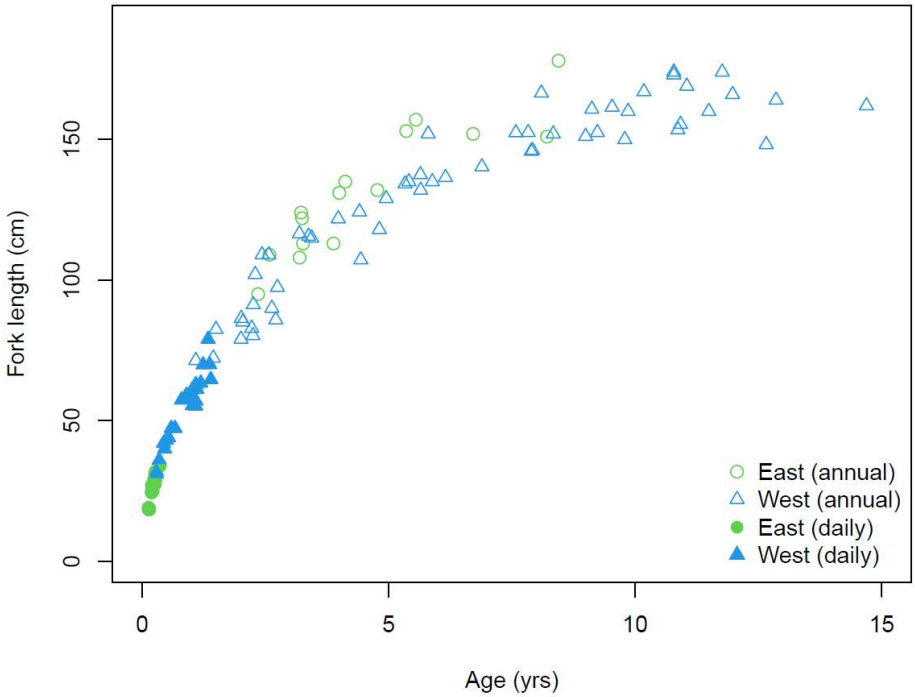

Append Figure 6: Length-at-age data for bigeye tuna caught east and west of 80°E in the Indian Ocean. There is some indication that bigeye in the west may grow slightly slower than bigeye in the east. However, the sample size is too small to be conclusive and other factors such as size-selective fishing could bias the data.

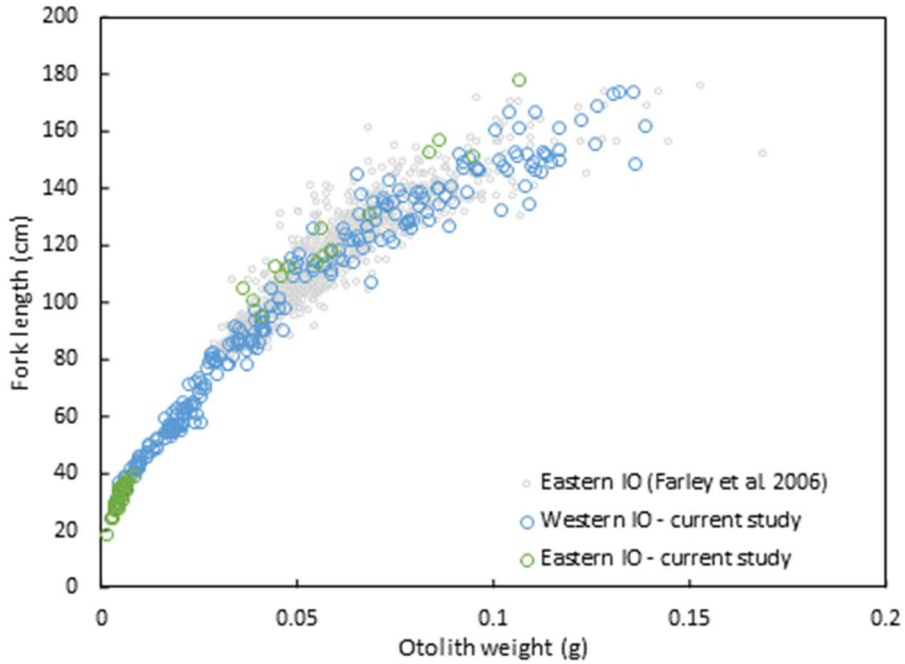

Append Figure 7. Relationship between otolith weight and fork length for bigeye tuna caught east and west of 80°E in the Indian Ocean from the current study and in the eastern Indian Ocean from Farley et al. (2006).

Appendix D – Comparison of age estimates

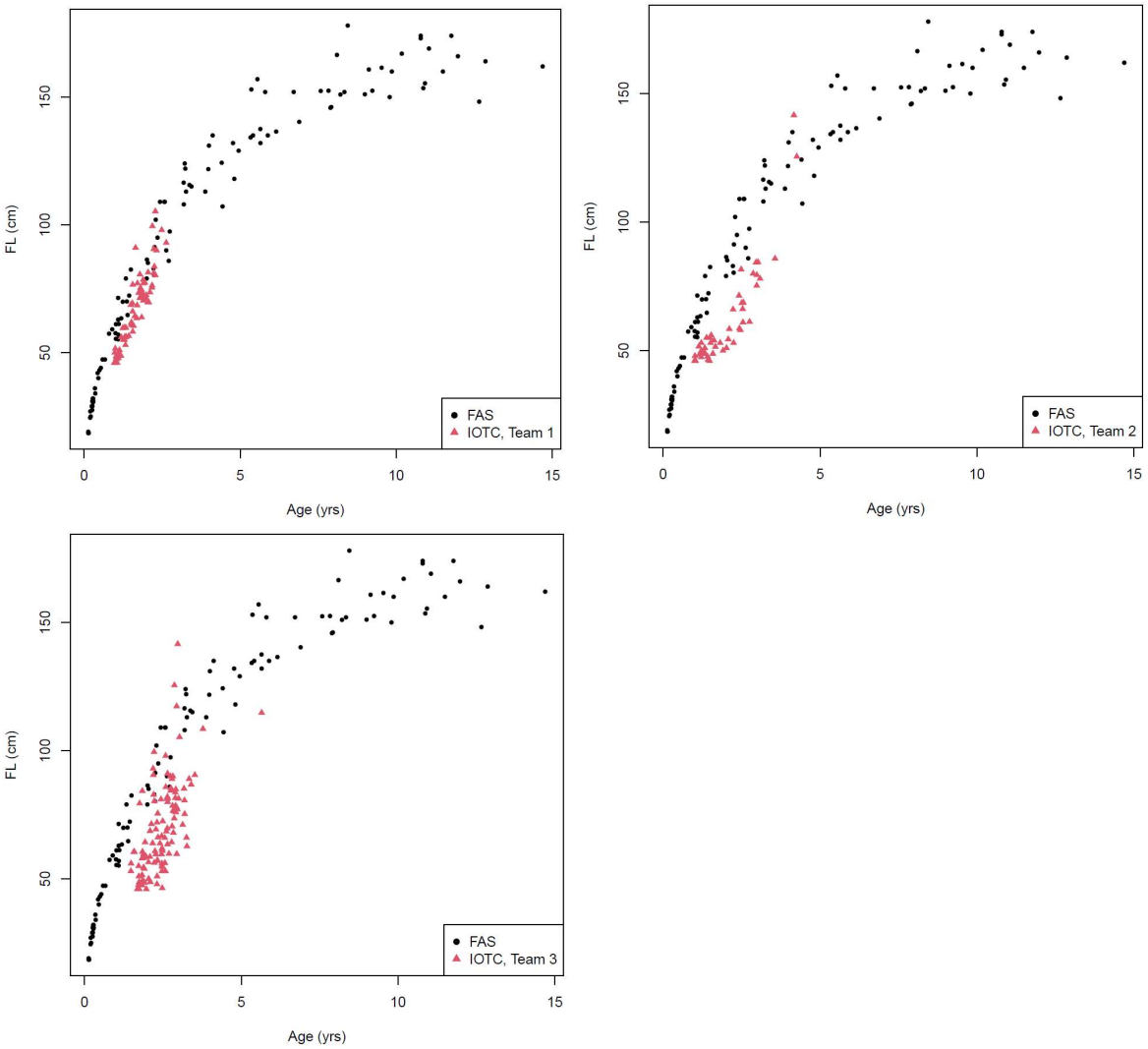

Append Figure 8. Comparison of age estimates obtained in the current study and daily age estimates obtained by reading Team 1, Team 2, and Team 3 in Sardenne et al. (2015).